

Beyond the WKB approximation in \mathcal{PT} -symmetric quantum mechanics

Patrick Dorey^{1,2}, Adam Millican-Slater¹ and Roberto Tateo³

¹*Dept. of Mathematical Sciences, University of Durham,
Durham DH1 3LE, United Kingdom*

²*Service de Physique Théorique, CEA-Saclay,
F-91191 Gif-sur-Yvette Cedex, France*

³*Dip. di Fisica Teorica and INFN, Università di Torino,
Via P. Giuria 1, 10125 Torino, Italy*

E-mails:

p.e.dorey@durham.ac.uk
adam.millican-slater@durham.ac.uk
tateo@to.infn.it

Abstract

The mergings of energy levels associated with the breaking of \mathcal{PT} symmetry in the model of Bender and Boettcher, and in its generalisation to incorporate a centrifugal term, are analysed in detail. Even though conventional WKB techniques fail, it is shown how the ODE/IM correspondence can be used to obtain a systematic approximation scheme which captures all previously-observed features. Nonperturbative effects turn out to play a crucial role, governing the behaviour of almost all levels once the symmetry-breaking transition has been passed. In addition, a novel treatment of the radial Schrödinger equation is used to recover the values of local and non-local conserved charges in the related integrable quantum field theories, without any need for resummation even when the angular momentum is nonzero.

1 Introduction

Following a paper by Bender and Boettcher [1], itself inspired by a conjecture of Bessis and Zinn-Justin [2], the subject of \mathcal{PT} -symmetric quantum mechanics has attracted growing interest. (A couple of earlier papers exploring related themes are [3, 4], while [5]–[23] provide a small sample of subsequent work.) Many studies have discussed general interpretational questions, but there are also mathematical issues to be addressed. One such is the topic of this paper: the pattern of \mathcal{PT} -symmetry breaking in the original model of Bender and Boettcher [1, 5], and in the generalisation of their model that was introduced in [8]. Numerical work has demonstrated an intriguing pattern of merging energy levels associated with the symmetry-breaking transition, but a complete analytic understanding has proved elusive, partly because standard WKB techniques break down in the regime where the symmetry-breaking occurs [1]. In this paper we show how this problem can be overcome, using a recently-discovered link with the theory of integrable quantum field theory [24] (the ‘ODE-IM correspondence’) to develop an approximation scheme for the energy levels which captures all features of the previously-observed behaviour in a controlled manner.

The remainder of this paper is organised as follows. Section 2 describes the symmetry-breaking transition in more detail, while section 3 discusses earlier theoretical treatments. The relevant connections with integrable quantum field theory are recalled in section 4, and then applied to the problem at hand in section 5. Section 6 then shows how a novel treatment of the radial anharmonic oscillator can be used to recover some of the results used earlier, calculations which may be of independent interest for the ODE-IM correspondence since they relate to the values of conserved charges in certain integrable quantum field theories. Finally, section 7 contains our conclusions.

2 Some \mathcal{PT} phenomenology

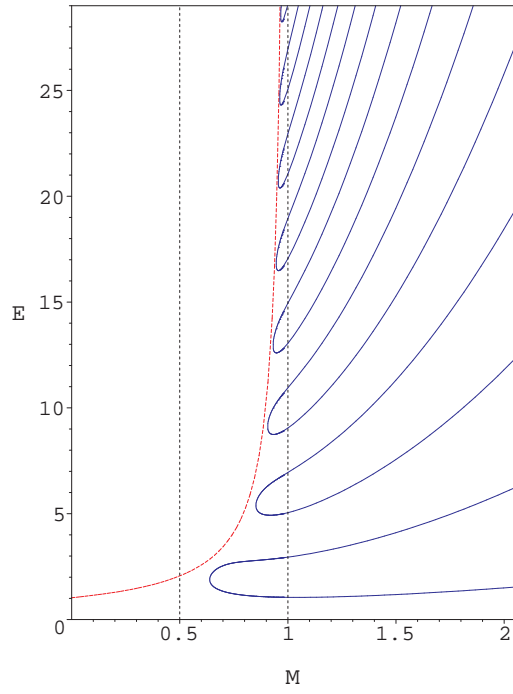
In the early 1990s, Bessis and Zinn-Justin [2] conjectured that the non-Hermitian Hamiltonian

$$\mathcal{H} = p^2 + i x^3 \tag{2.1}$$

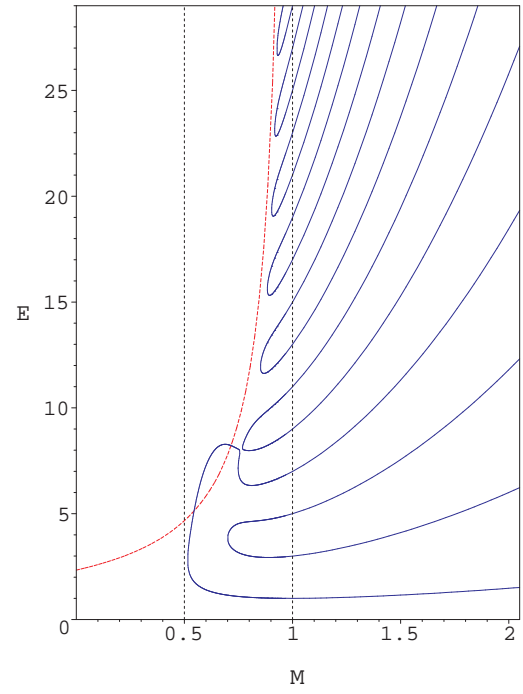
should have a real and positive spectrum, if the boundary condition $\psi \in L^2(\mathbb{R})$ is imposed on the position-space wavefunctions $\psi(x)$. This initially-surprising proposal was motivated by considerations of the quantum field theory of the Lee-Yang model; it was subsequently put into a more directly quantum-mechanical context by Bender and Boettcher [1], who also suggested that the spectral properties of the one-parameter family of Hamiltonians

$$\mathcal{H}_M = p^2 - (ix)^{2M} \tag{2.2}$$

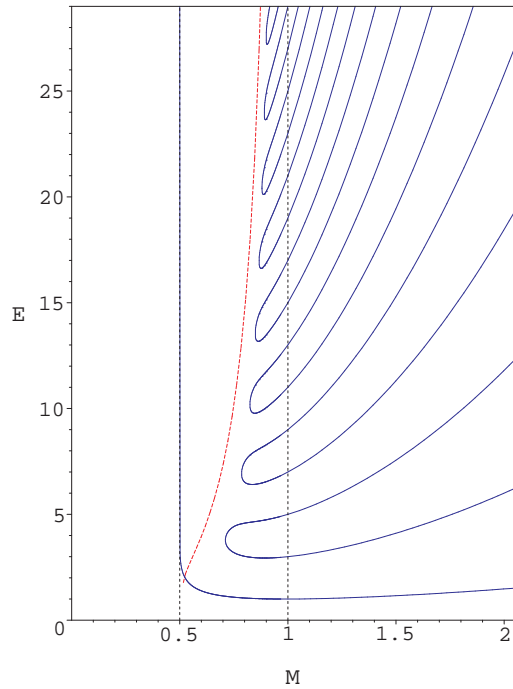
might be of interest, with M a positive real number. Varying M from $3/2$ to 1 interpolates between $\mathcal{H}_{3/2}$, the Bessis–Zinn-Justin Hamiltonian, and \mathcal{H}_1 , the much more familiar Hamiltonian of the simple harmonic oscillator. For $M \geq 2$, analytic continuation (in M) of the eigenvalue problem requires boundary conditions to be imposed on a suitably-chosen contour in the complex plane, away from the real axis [1]; given this, Bender and Boettcher found that the conjecture of Bessis and Zinn-Justin could be strengthened to the statement that the spectrum of \mathcal{H}_M is real and positive for all $M \geq 1$. This reality property is associated with, but not completely explained by, the so-called \mathcal{PT} symmetry of the corresponding spectral problems. In fact, it is only recently that a complete proof of the Bender-Boettcher conjecture has been given [10].



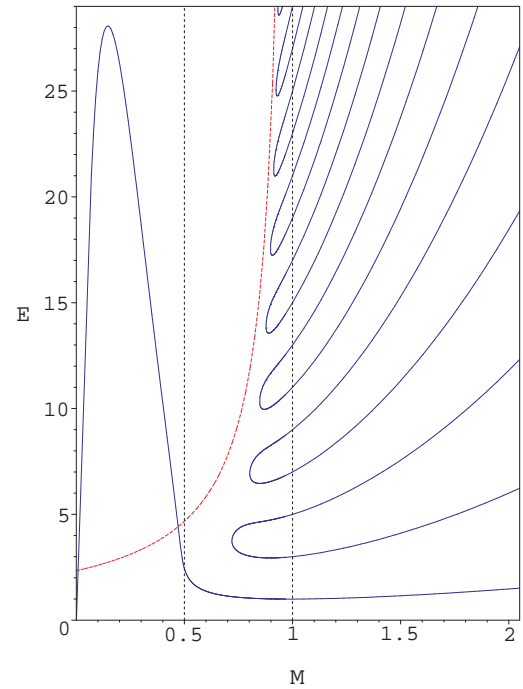
1a: $l = -0.025$



1b: $l = -0.001$



1c: $l = 0$



1d: $l = 0.001$

Figure 1: Real eigenvalues of $p^2 - (ix)^{2M} + l(l+1)/x^2$ as functions of M , for various values of l . The (curved) dotted lines show the asymptotic locations of the level-mergings, to be discussed in section 5 below.

Most interesting, though, is the behaviour of the spectrum as M falls below 1, shown in figure 1c. Numerical results indicate that infinitely-many eigenvalues collide in pairs and

become complex, leaving a finite number of real eigenvalues [1]. As M decreases further, these successively pair off and become complex until finally the second and third levels merge and only the ground state remains real, which itself diverges to infinity as $M \rightarrow \frac{1}{2}^+$. (For $M = \frac{1}{2}$, the spectrum of (2.2) is null, as can be seen by shifting ix to $ix - E$ and solving the differential equation using the Airy function.)

The mysterious nature of the transition at $M = 1$ is highlighted by a further generalisation of Bessis and Zinn-Justin's Hamiltonian, to incorporate an additional 'angular momentum' term [8]:

$$\mathcal{H}_{M,l} = p^2 - (ix)^{2M} + \frac{l(l+1)}{x^2}. \quad (2.3)$$

Here l is a real parameter, which can be assumed no smaller than $-1/2$, since the problem is unchanged by the replacement of l by $-1-l$. For $l \neq 0$, the contour on which the wavefunction is defined should be distorted below the singularity at $x = 0$, in addition to any distortions away from the real axis required for $M \geq 2$. The spectrum of $\mathcal{H}_{M,l}$ is then real for all $M \geq 1$, and positive if in addition $l < M/2$ [10]. As before, there is a transition at $M = 1$, with infinitely-many levels becoming complex. However, as illustrated in figure 1a, for sufficiently-negative values of l there is a remarkable change in the way that the remaining real levels pair off: the parity is reversed, so that the second level is paired not with the third level, but rather with the ground state, and so on up the spectrum. This reversed pairing holds true for sufficiently-high levels for all negative l , but as l gets closer to zero the level with which the ground state is paired moves up through the spectrum, leaving the connectivity of the original Bender-Boettcher problem in its wake and allowing for a continuous transition to the previous behaviour at $l = 0$. This is described at greater length in [8], and is best understood by looking at figures 1a – 1d, or at figure 2 of [8]; the challenge is to obtain an analytic understanding of why it occurs.

3 Some \mathcal{PT} Theory

A first insight into the phenomena described in the last section comes from the observation that, while \mathcal{H}_M is not Hermitian in any simple sense, it *is* invariant under the combined action of the operators \mathcal{P} and \mathcal{T} [1], where \mathcal{P} is parity and \mathcal{T} time reversal, acting on Schrödinger potentials $V(x)$ as

$$\mathcal{P}V(x)\mathcal{P}^{-1} = V(-x^*) \quad , \quad \mathcal{T}V(x)\mathcal{T}^{-1} = V(x)^* \quad . \quad (3.1)$$

(The complex conjugation in the definition of parity ensures that the deformed contours required for $M \geq 2$ are mapped onto themselves, but is otherwise unimportant.) As shown in [5], \mathcal{PT} invariance implies that eigenvalues are either real, or come in complex-conjugate pairs, much like the roots of a real polynomial (see also [20]). Real eigenvalues correspond to wavefunctions symmetrical under \mathcal{PT} , complex eigenvalues to a spontaneous breaking of this symmetry. In contrast to Hermiticity, on its own \mathcal{PT} symmetry is not enough to prove reality; but it does mean that if a level is to become complex, then it must pair off with some other real level first.

To deal with the transition at $M = 1$, Bender, Boettcher and Meisinger [5] used a basis of the exactly-known eigenfunctions $|n\rangle$ of \mathcal{H}_1 , the simple Harmonic oscillator:

$$\mathcal{H}_1|n\rangle = (2n+1)|n\rangle \quad , \quad n = 0, 1, \dots \quad (3.2)$$

and approximated the Hamiltonian for small $\epsilon := 2(M-1)$ as

$$\mathcal{H}_{1+\epsilon/2} = p^2 + x^2 + \epsilon x^2 \left[\ln|x| + \frac{i\pi}{2} \text{sgn}(x) \right] + O(\epsilon^2). \quad (3.3)$$

Truncating the approximate Hamiltonian to the two-dimensional subspace spanned by $|2n-1\rangle$ and $|2n\rangle$, for large n and small ϵ the matrix elements are [5]

$$\mathcal{H}_{\text{trunc}} \approx \begin{pmatrix} a(2n-1) & ib(2n) \\ ib(2n) & a(2n) \end{pmatrix} \quad (3.4)$$

where

$$a(n) = 2n + 1 + \frac{\epsilon n}{2} \ln(n) \quad , \quad b(n) = \frac{4}{3} \epsilon n . \quad (3.5)$$

Diagonalising $\mathcal{H}_{\text{trunc}}$ yields the prediction that the energy levels of $\mathcal{H}_{1+\epsilon/2}$ should join and become complex for

$$|\epsilon| \sim \frac{3}{8n} , \quad (3.6)$$

matching the numerical observation that the points at which levels merge approach the line $M = 1$ as the level n tends to infinity.

However, the agreement of this result with the numerical data is only qualitative, and even at this level, there are problems. Firstly, the approximation also predicts a merging of levels for *positive* values of ϵ , which is clearly wrong; and secondly, if one instead truncates to the subspace spanned by the levels $|2n\rangle$ and $|2n+1\rangle$, then the same approximation predicts that these two levels should pinch off. As underlined by the effect of the angular-momentum term, it is by no means obvious *a priori* how the pairing of levels should go, and it is reasonable to demand that any full understanding of the transition at $M = 1$ should include a robust (and correct!) prediction on this point. Figures 2a and 2b illustrate the situation.

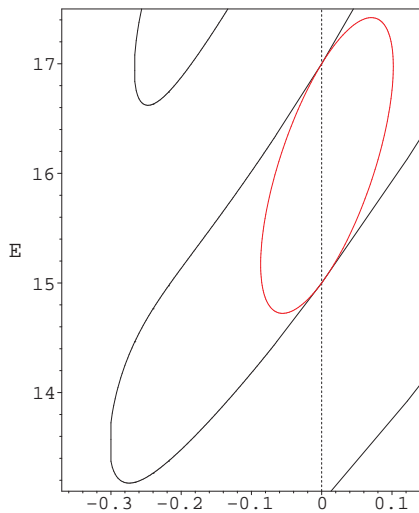


Figure 2a: Truncation to levels 8 and 9, compared with numerical data

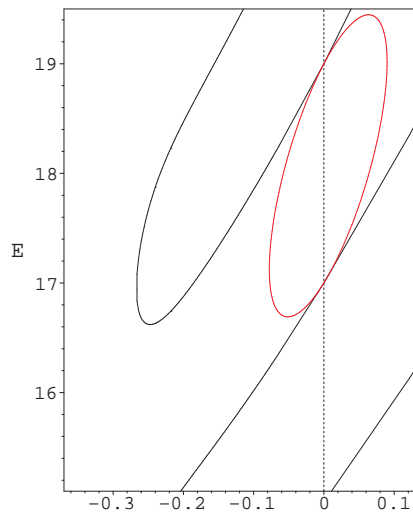


Figure 2b: Truncation to levels 9 and 10, compared with numerical data

The discussion of [5] concerned the zero angular-momentum case. Since this is on the boundary between the two sorts of level connectivity, one might hope for a clearer signal from the truncated Hamiltonian at $l \neq 0$, where the matrix elements can be given in terms of hypergeometric functions. However, we have found that the problems described above persist.

The approximation (both for zero and for non-zero angular momentum) does improve if the dimension of the truncated subspace is increased, but this rapidly reverts to a numerical treatment, and any analytical understanding is lost. Alternatively, it might be hoped that the full set of matrix elements in the harmonic oscillator basis would simplify sufficiently in a suitable large- n , small- ϵ limit that a precise prediction could be made. While this seems a technically-interesting avenue to explore, it is a delicate exercise to extract the relevant asymptotics, and we have yet to make useful progress in this direction.

In more standard quantum-mechanical problems, methods such as truncation are not necessary when discussing the asymptotic behaviour of the high-lying levels, as the WKB approximation can be used. Indeed, this method gives very accurate results for the current problem when $M \geq 1$ [1]. However, the direct application of WKB *fails* for $M < 1$ [1]: the path along which the phase-integral quantization condition should be taken crosses a cut and ceases to join the relevant two turning points. A naïve analytic continuation of the WKB results for $M \geq 1$ to $M < 1$ also fails, producing energy levels which do not even become complex.

In the following we shall show how these problems can be avoided, by developing an approximation scheme using the so-called ODE/IM correspondence, which links the Bender-Boettcher problem and its generalisations to a set of integrable quantum field theories associated with the sine-Gordon model. For $M \geq 1$ the WKB approximation is recovered, but for $M < 1$ the results are significantly different. In preparation, the next section gives a brief review of the correspondence.

4 More \mathcal{PT} Theory: the ODE/IM correspondence

In its simplest form, the ODE/IM correspondence links the spectral properties of certain Schrödinger equations to functions which appear in the study of integrable quantum field theories in 1+1 dimensions. The phenomenon was first observed in [24], for Schrödinger problems with homogeneous potentials $V(x) = x^{2M}$. The correspondence was generalised to incorporate an additional angular-momentum like term in [25] and a more general potential in [26], while its relevance to the non-Hermitian spectral problems of \mathcal{PT} -symmetric quantum mechanics was found in [8]. A longer review of the subject is given in [27], and here we shall just summarise the key results, largely following [8].

Let $\{E_i\}$ be the set of eigenvalues of $\mathcal{H}_{M,l}$, defined in (2.3), and let $\{e_j\}$ be the eigenvalues of a similar-looking but Hermitian problem

$$\left(-\frac{d^2}{dx^2} + x^{2M} + \frac{l(l+1)}{x^2}\right)\psi = E\psi \quad (4.1)$$

with so-called ‘radial’ boundary conditions $\psi(x) = O(x^{l+1})$ as $x \rightarrow 0$, $\psi(x) \rightarrow 0$ as $x \rightarrow \infty$. (Correspondingly, the earlier, \mathcal{PT} -symmetric problems are sometimes said to have ‘lateral’ boundary conditions.) A pair of spectral determinants for these two problems, $T(E)$ and $Q(E)$, can be defined as follows. For any E , not necessarily an eigenvalue of either problem, let $y(x, E, l)$ be the unique solution to (4.1) which has the same asymptotic as $x \rightarrow +\infty$ on the real axis as

$$y^{\text{WKB}}(x, E) := \frac{1}{\sqrt{2i}} P(x)^{-1/4} \exp\left(-\int_0^x \sqrt{P(t)} dt\right) \quad (4.2)$$

where $P(x) = x^{2M} - E$. (Note, so long as M is positive, l is not involved in the specification

of this asymptotic.) To give some examples:

$$M > 1: \quad y(x, E, l) \sim \frac{1}{\sqrt{2i}} x^{-M/2} \exp\left(-\frac{1}{M+1} x^{M+1}\right) \quad (4.3)$$

$$M = 1: \quad y(x, E, l) \sim \frac{1}{\sqrt{2i}} x^{-1/2+E/2} \exp\left(-\frac{1}{2} x^2\right) \quad (4.4)$$

$$1 > M > \frac{1}{3}: \quad y(x, E, l) \sim \frac{1}{\sqrt{2i}} x^{-M/2} \exp\left(-\frac{1}{M+1} x^{M+1} + \frac{E}{2-2M} x^{1-M}\right) \quad (4.5)$$

More generally, the explicit asymptotic of $y(x, E, l)$ changes whenever $M = 1/(2m-1)$ with m a positive integer, as is easily seen from (4.2). We also define $\psi(x, E, l)$ to be the solution to (4.1) which behaves as $x \rightarrow 0$ as

$$\psi(x, E, l) \sim x^{l+1} + O(x^{l+3}). \quad (4.6)$$

Here we continue to take $\Re l \geq -1/2$, making the definition unique; if desired, a second solution $\psi(x, E, -1-l)$ to (4.1) can be uniquely specified by analytic continuation in l .

Denoting the Wronskian $fg' - f'g$ of two functions $f(x)$ and $g(x)$ by $W[f, g]$, we now define T and Q by

$$T(E) := W[y(\omega x, \omega^{-2}E, l), y(\omega^{-1}x, \omega^2E, l)] \quad (4.7)$$

$$Q(E) := W[y(x, E, l), \psi(x, E, l)] \quad (4.8)$$

where

$$\omega = e^{i\pi/(M+1)}. \quad (4.9)$$

Then it is straightforwardly shown [8] that the zeroes of T are exactly the points $\{-E_i\}$, and the zeroes of Q are the points $\{e_j\}$, so these two functions are indeed spectral determinants. Furthermore they obey the following functional relation:

$$T(E)Q(E) = \omega^{-l-1/2} Q(\omega^{-2}E) + \omega^{l+1/2} Q(\omega^2E) \quad (4.10)$$

which is the same as Baxter's T-Q relation [28] from the theory of integrable lattice models, in the form which arises in connection with the quantum field theory of the massless sine-Gordon model [29]. (Strictly speaking, for $l \neq -1/2$, Q as defined here corresponds to the function denoted A in [29].) At the points $M = 1/(2m-1)$ where the asymptotic form of y changes, a correction term appears in (4.10) [29, 8], but the only case potentially relevant in the following is $M = m = 1$, to which we shall return briefly below.

Now define

$$a(E) := \omega^{2l+1} \frac{Q(\omega^2E)}{Q(\omega^{-2}E)}. \quad (4.11)$$

By (4.10), $a(E) = -1$ precisely at the zeroes of $T(E)$ and $Q(E)$, that is at the set of points $\{-E_i\} \cup \{e_j\}^*$. Furthermore, provided the $\{e_j\}$ lie on the positive real axis and the $\{-E_i\}$ lie away from it, $a(E)$ can be found by solving a nonlinear integral equation, as follows [30, 31, 29]. Trade E for a 'rapidity' $\theta(E)$, such that

$$E^{(M+1)/(2M)} = r e^\theta. \quad (4.12)$$

*Note, exceptionally, the zeroes of the LHS of (4.10) might coincide with simultaneous zeroes of the factors on the RHS, but this will not concern us below.

Then, for $|\Im m \theta| < \min(\pi, \pi/M)$, the ‘counting function’

$$f(\theta) := \log a(E(\theta)) \quad (4.13)$$

solves

$$\begin{aligned} f(\theta) = & i\pi(l + \frac{1}{2}) - imre^\theta + \int_{C_1} \varphi(\theta - \theta') \log(1 + e^{f(\theta')}) d\theta' \\ & - \int_{C_2} \varphi(\theta - \theta') \log(1 + e^{-f(\theta')}) d\theta' \end{aligned} \quad (4.14)$$

where

$$m = \sqrt{\pi} \frac{\Gamma(1 + \frac{1}{2M})}{\Gamma(\frac{3}{2} + \frac{1}{2M})} = \frac{1}{M} B(\frac{3}{2}, \frac{1}{2M}) \quad (4.15)$$

and

$$B(p, q) = \frac{\Gamma(p)\Gamma(q)}{\Gamma(p+q)} = \int_0^1 t^{p-1}(1-t)^{q-1} dt \quad (4.16)$$

is Euler’s beta function. The integration contours C_1 and C_2 in (4.14) run from $-\infty$ to $+\infty$ just below and just above the real axis, close enough that all of the points $\{\theta(e_j)\}$, and none of the points $\{\theta(-E_i)\}$, lie between C_1 and C_2 , and the kernel function $\varphi(\theta)$ is

$$\varphi(\theta) = \int_{-\infty}^{\infty} e^{ik\theta} \frac{\sinh(\frac{\pi}{2} \frac{1-M}{M} k)}{2 \cosh(\frac{\pi}{2} k) \sinh(\frac{\pi}{2M} k)} \frac{dk}{2\pi}. \quad (4.17)$$

The value of the normalisation factor r is arbitrary, but to match the conventions of [29, 8] one should take

$$r = (2M+2) \Gamma\left(\frac{M}{M+1}\right)^{(M+1)/M}. \quad (4.18)$$

The nonlinear integral equation (4.14) must be modified if any $\theta(e_j)$ moves outside the contours C_1 and C_2 [29], or if any $\theta(-E_i)$ moves inside them [32]. However these possibilities do not arise in the current context, at least for small values of l : for $M \geq 1$ and $|2l+1| < M+1$ it can be shown that all of the e_j lie on the positive real axis of the complex E plane, and all of the $-E_i$ on the negative real axis (see [8, 10]). For $M < 1$, the arguments showing that the $\{e_j\}$ lie on the positive real axis continue to hold, but, as we already saw, the $\{-E_j\}$ do move away from the negative real axis and become complex. However, our numerical results show clearly that they never become near enough to the real axis to upset the arguments below.

5 Asymptotics from the integral equation

Equation (4.14) provides an effective way to solve the radial spectral problem (4.1) [24]: given that the zeroes of T all lie away from the positive real E axis, any point on the real θ axis at which $f(\theta) = (2n+1)\pi i$ for some $n \in \mathbb{Z}$ must correspond to a zero of Q . The values of $f(\theta)$ on C_1 and C_2 can be obtained numerically from (4.14) by a simple iterative procedure, after which the same equation can be used to obtain $f(\theta)$ on the real axis, allowing those points at which $f(\theta) = (2n+1)\pi i$ to be located with high accuracy. The leading approximation for $f(\theta)$, found by dropping the integrals from (4.14), yields the usual WKB result; higher corrections can be obtained using the asymptotic expansion for $Q(E)$ in terms of local and non-local charges given in [29, 33].

The same numerical approach was used in [8] to analyse the non-Hermitian spectral problems based on (2.3); it was also used to generate figure 1 above. However an analysis of the implications for the asymptotic behaviour of the energy levels was not given. Compared to the Hermitian case, there are a number of subtleties, which we now discuss.

The first point, which was already taken into account in the numerical work described in [8], is that the zeroes of $T(E)$ are either on or near to the *negative* real E -axis, which is the line $\Im m \theta = \pi(M+1)/(2M)$ on the complex θ -plane. Since $(M+1)/(2M) > \min(1, 1/M)$ for all $M \neq 1$, this means that the relevant values of $f(\theta)$ lie outside the strip described by (4.14). Instead, the so-called ‘second determination’ must be used [34]. This arises because the kernel $\varphi(\theta)$ has, amongst others, poles at $\theta = \pm i\pi$ and $\pm i\pi/M$, which add residue terms to the analytic continuation (4.14) outside the strip $|\Im m \theta| < \min(\pi, \pi/M)$. (See [35] for related discussions in the context of the thermodynamic Bethe ansatz.)

For $M > 1$ (sometimes called the attractive, or semiclassical, regime in the quantum field theory context) the poles in $\varphi(\theta)$ nearest to the real axis are at $\theta = \pm i\pi/M$, and have residue $-\frac{1}{2\pi i}$. Increasing $\Im m \theta$ past π/M , the pole at $\theta = -i\pi/M$ crosses C_1 and then C_2 , generating a term $-f(\theta - i\pi/M)$ which should be added to the right-hand side of (4.14) in order to give a correct representation of $f(\theta)$ for $\Im m \theta$ just greater than π/M . Using the original representation (4.14) to rewrite the extra term, the resulting expression is

$$f(\theta) = -i(1 - e^{-i\pi/M}) m r e^\theta + \int_{C_1} \varphi_{II}(\theta - \theta') \log(1 + e^{f(\theta')}) d\theta' - \int_{C_2} \varphi_{II}(\theta - \theta') \log(1 + e^{-f(\theta')}) d\theta' \quad (5.1)$$

where

$$\varphi_{II}(\theta) = \varphi(\theta) - \varphi(\theta - i\pi/M) = \frac{2i \cos(\frac{\pi}{2M}) \sinh(\theta - \frac{i\pi}{2M})}{\pi(\cosh(2\theta - \frac{i\pi}{M}) - \cos(\frac{\pi}{M}))}. \quad (5.2)$$

An examination of the poles in $\varphi_{II}(\theta)$ shows that (5.1) holds for $\pi/M < \Im m \theta < \pi$, which includes the neighbourhood of the line $\Im m \theta = \pi(M+1)/(2M)$ relevant to the hunt for the zeroes of $T(E)$. (For simplicity we have supposed that C_1 and C_2 are infinitesimally close to the real axis; otherwise an ‘intermediate determination’ is also required, applying when the pole in $\varphi(\theta)$ has crossed C_1 but not C_2 .)

For $M < 1$ (the ‘repulsive regime’ in quantum field theory language) the nearest poles are instead at $\theta = \pm i\pi$, and for $\Im m \theta > \pi$ the extra term to be added to the right-hand side of (4.14) is equal to $+f(\theta - i\pi)$. Rewriting using the original representation as before, one finds

$$f(\theta) = 2i\pi(l + \frac{1}{2}) + \int_{C_1} \varphi_{II}(\theta - \theta') \log(1 + e^{f(\theta')}) d\theta' - \int_{C_2} \varphi_{II}(\theta - \theta') \log(1 + e^{-f(\theta')}) d\theta' \quad (5.3)$$

where

$$\varphi_{II}(\theta) = \varphi(\theta) + \varphi(\theta - i\pi) = \frac{M \sin(\pi M)}{\pi(\cosh(2M\theta - i\pi M) - \cos(\pi M))}. \quad (5.4)$$

This holds for $\pi < \Im m \theta < \pi/M$.

The goal is to locate the zeroes of $T(E)$ on or near the negative- E axis. To this end we set $\theta = i\pi(M+1)/(2M) + \gamma$, define the shifted counting function

$$g(\gamma) := f(i\pi(M+1)/(2M) + \gamma) \quad (5.5)$$

Abusing the notation a little, we shall sometimes write g as a function of the energy E , $g(E) := f(-E)$, where

$$E = (re^\gamma)^{2M/(M+1)}. \quad (5.6)$$

The eigenvalues of the \mathcal{PT} -symmetric problem (2.3) are then those values of E such that

$$g(E) = (2k+1)\pi i \quad (5.7)$$

for some $k \in \mathbb{Z}$.

Defining $\psi(\gamma) := \varphi_{II}(i\pi(M+1)/(2M) + \gamma)$, $g(\gamma)$ is given exactly, for $|\Im m \gamma| < \frac{\pi}{2}|\frac{M-1}{M}|$, by the following expressions:

$M > 1$:

$$\begin{aligned} g(\gamma) = & 2i \sin\left(\frac{\pi}{2M}\right) m r e^\gamma + \int_{C_1} \psi(\gamma - \theta') \log(1 + e^{f(\theta')}) d\theta' \\ & - \int_{C_2} \psi(\gamma - \theta') \log(1 + e^{-f(\theta')}) d\theta' \end{aligned} \quad (5.8)$$

with

$$\psi(\gamma) = \frac{2 \cos\left(\frac{\pi}{2M}\right) \cosh(\gamma)}{\pi(\cosh(2\gamma) + \cos\left(\frac{\pi}{M}\right))} = \sum_{n=1}^{\infty} (-1)^{n+1} \frac{2}{\pi} \cos\left(\frac{\pi}{2M}(2n-1)\right) e^{-(2n-1)\gamma}. \quad (5.9)$$

$M < 1$:

$$\begin{aligned} g(\gamma) = & 2i\pi(l + \frac{1}{2}) + \int_{C_1} \psi(\gamma - \theta') \log(1 + e^{f(\theta')}) d\theta' \\ & - \int_{C_2} \psi(\gamma - \theta') \log(1 + e^{-f(\theta')}) d\theta' \end{aligned} \quad (5.10)$$

with

$$\psi(\gamma) = \frac{-M \sin(\pi M)}{\pi(\cosh(2M\gamma) + \cos(\pi M))} = \sum_{n=1}^{\infty} (-1)^n \frac{2M}{\pi} \sin(\pi M n) e^{-2Mn\gamma}. \quad (5.11)$$

(We have recorded the large- γ expansions for ψ as they will be needed later.)

The formulae (5.8) and (5.10) express $g(\gamma)$ in terms of the values of $f(\theta')$ on the contours C_1 and C_2 , where the original ('first determination') specification (4.14) applies. For a given value of γ , the dominant contributions to the integrals in (5.8) and (5.10) come when $\Re e \theta' \approx \Re e \gamma$, since the kernel $\psi(\gamma)$ is peaked about $\gamma = 0$. For large $\Re e \theta'$ on C_1 and C_2 , $f(\theta') \sim i\pi(l+1) - imre^{\theta'}$. Since C_1 is just below the real axis, and C_2 just above, in this limit $\log(1 + e^{f(\theta')}) \rightarrow 0$ on C_1 , and $\log(1 + e^{-f(\theta')}) \rightarrow 0$ on C_2 . Therefore, for large $\Re e \gamma$ the integrals in (5.8) and (5.10) can be dropped, giving the following leading approximations[†] for $g(\gamma)$:

$$M > 1 : \quad g(\gamma) \sim 2i \sin\left(\frac{\pi}{2M}\right) m E^{\frac{(M+1)}{2M}} \quad (5.12)$$

$$M = 1 : \quad g(\gamma) = i\pi(l + \frac{1}{2}) + i\frac{\pi}{2} E \quad (5.13)$$

$$M < 1 : \quad g(\gamma) \sim 2i\pi(l + \frac{1}{2}) \quad (5.14)$$

[†]The result for $M = 1$, which is exact, follows directly from (4.14) since $\varphi(\theta) \equiv 0$ in this case and no second determination is required. Since $m|_{M=1} = \pi/2$, it interpolates between the results for $M = 1^+$ and $M = 1^-$. This interpolation will be discussed in more detail around equation (5.31) below.

For $M > 1$, the leading approximation for the energy levels is obtained by setting the RHS of (5.12) equal to $(2n+1)\pi i$. Then, using (4.15), the WKB result of [1, 5] is recovered:

$$E_n \sim \left(\frac{\sqrt{\pi} \Gamma(\frac{3}{2} + \frac{1}{2M}) (n + \frac{1}{2})}{\sin(\frac{\pi}{2M}) \Gamma(1 + \frac{1}{2M})} \right)^{2M/(M+1)}. \quad (5.15)$$

For $M = 1$, there are some subtleties. Since the eigenvalues at this point are easily found exactly, they can be ignored, but their resolution is perhaps interesting. At $M = 1$, $\omega = i$ and the factors $Q(\omega^{\pm 2})$ in (4.11) cancel, making f and g as naively defined by (4.13) and (5.5) equal to $\pi(l + \frac{1}{2})$. However this is too quick: at $M = 1$ the TQ relation (4.10) is ‘renormalised’ to $T(E)Q(E) = \omega^{-l-1/2+E/2} Q(\omega^{-2}E) + \omega^{l+1/2-E/2} Q(\omega^2E)$ [29, 8], and as a result (4.11) is naturally replaced by $a(E) = \omega^{2l+1-E} Q(\omega^2E)/Q(\omega^{-2}E)$, which indeed matches (5.13). Next, the renormalised TQ relation implies $T(E)Q(E) = 2 \cos((2l+1-E)\pi/4)Q(-E)$. Knowing that the zeroes of Q are positive and those of T negative allows this relation to be disentangled: the zeroes of Q must be at $E = 2l - 1 + 4n$, and those of T at $E = 2l + 3 - 4n$ and $-2l + 1 - 4n$, for $n = 1, 2, \dots$. Recalling that the eigenvalues of the lateral problem are at the negated zeroes of T recovers the spectrum of the ‘PT-symmetric simple harmonic oscillator’, previously obtained in [6] and [8] via explicit solutions of the differential equation.

Finally, for $M < 1$ the leading approximation to $g(\gamma)$ is a constant, and does not give any information about the energy levels at all. This gives a novel insight into the observation of [1] that standard WKB techniques fail for $M < 1$: from the point of view of the ODE/IM correspondence and its associated nonlinear integral equation, it can be traced to the change in the nature of the second determination in the repulsive regime.

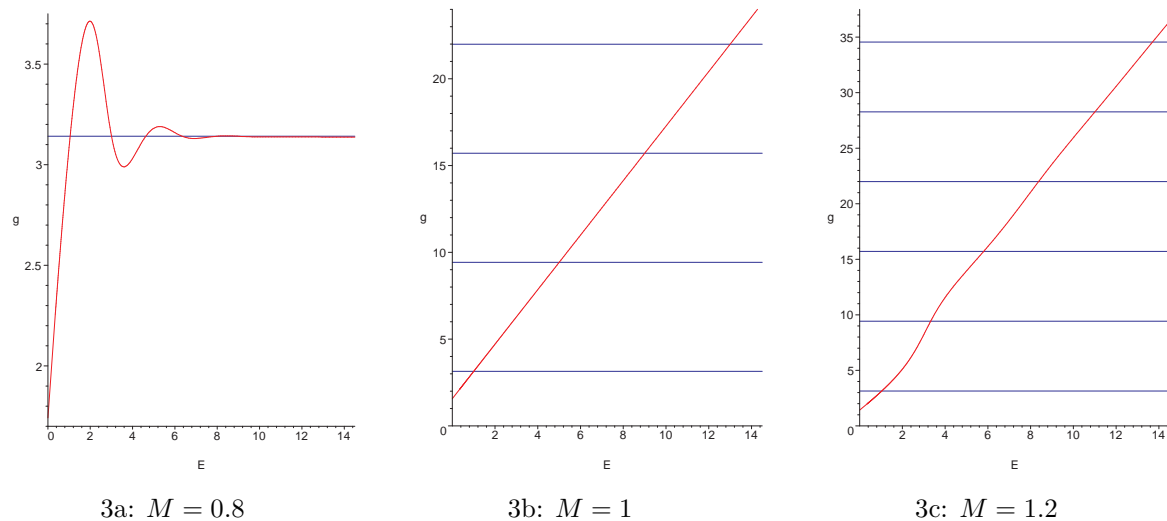


Figure 3: $\Im m g(E)$ from the nonlinear integral equation. In all three cases, $l = -0.001$. The horizontal lines show the ‘quantisation levels’ $g = (2n+1)\pi i$.

To proceed further, the more detailed behaviour of $g(E)$ is required. Figure 3 shows $\Im m g(E)$ in the various regimes, the plots being obtained by solving the NLIE numerically, but with no other approximations. Note that the nature of the energy level quantisation is radically changed for $M < 1$: even for the levels which are still real, there is no natural way to allot them a unique WKB (Bohr-Sommerfeld) quantum number via the counting function, as happens for standard eigenvalue problems in quantum mechanics, and also for these lateral (\mathcal{PT} -symmetric) problems when $M > 1$.

The next task is to understand figure 3 analytically. It turns out that the direct use of the asymptotic expansion for $Q(E)$ developed in [29, 33] fails to capture most of the important features of the energy levels for $M < 1$: roughly put, the wiggles in figure 3a are missed, and the asymptotic behaviour of just a single level is captured – the partner of the ground state, which moves up to infinity as $l \rightarrow 0^-$ (this can be seen on figure 1b, and is illustrated in more detail in figure 5a below). The remaining levels only emerge when a ‘beyond all orders’ term is added. The need for this term is most easily understood if we continue to work directly with the nonlinear integral equation.

Higher corrections to $g(\gamma)$ can be obtained through a steepest-descent treatment of the integrals in (5.8) or (5.10), expanding the kernels $\psi(\gamma - \theta')$ for large $\gamma - \theta'$ and using again the fact that the terms $\log(1 + e^{f(\theta')})$ and $\log(1 + e^{-f(\theta')})$ decay to zero as $\Re \theta' \rightarrow \infty$ along C_1 and C_2 respectively. This requires the contours C_1 and C_2 to be shifted so as to maximise the rates of decay of $\log(1 + e^{\pm f(\theta')})$ along them. For large $\Re \theta'$ with $|\Im m \theta'| < \min(\pi, \pi/M)$, $f(\theta') \sim i\pi(l + \frac{1}{2}) - imre^{\theta'}$, so C_1 should be shifted down to $\Im m \theta' = -\pi/2$, and C_2 shifted up to $\Im m \theta' = +\pi/2$. (For $M < 2$, these lines do indeed lie inside the first determination, for which the just-mentioned asymptotic of $f(\theta')$ holds, and we restrict to such cases in the following.) These shifts of contours are not entirely innocent operations, as the kernel functions $\psi(\gamma)$ have poles at $\gamma = \pm \frac{i\pi}{2} \frac{|M-1|}{M}$. Taking C_1 and C_2 past these poles generates residue terms proportional to the values of $\log(1 + e^{\pm f(\theta')})$ there. These are the ‘beyond all orders’ terms just advertised.

Explicitly, let \tilde{C}_1 and \tilde{C}_2 be the contours C_1 and C_2 shifted onto the steepest descent (for large $\Re \theta'$) paths $\Im m \theta' = -\pi/2$ and $\Im m \theta' = +\pi/2$ respectively. For $1 < M < 2$, (5.8) can then be rewritten as

$$\begin{aligned} g(\gamma) &= 2i \sin\left(\frac{\pi}{2M}\right) mre^\gamma \\ &+ \int_{\tilde{C}_1} \psi(\gamma - \theta') \log(1 + e^{f(\theta')}) d\theta' - \int_{\tilde{C}_2} \psi(\gamma - \theta') \log(1 + e^{-f(\theta')}) d\theta' \\ &+ \log(1 + e^{f(\gamma - \frac{\pi i}{2} \frac{|M-1|}{M})}) - \log(1 + e^{-f(\gamma + \frac{\pi i}{2} \frac{|M-1|}{M})}). \end{aligned} \quad (5.16)$$

For $\frac{1}{2} < M < 1$, the representation (5.10) is rewritten in a similar manner, modulo a change in the signs of the extra terms, due to the opposite residues of the relevant poles. (For $M < \frac{1}{2}$, the poles are not encountered in the shifting of C_1 and C_2 , and so no extra terms are needed.)

Once the contours have been shifted, the kernel functions are expanded using (5.9) and (5.11) to give asymptotic expansions of the integrals in the standard way. Setting $E = (re^\gamma)^{2M/(M+1)}$, for $1 < M < 2$ this yields

$$\begin{aligned} g(E) &\sim 2i \sin\left(\frac{\pi}{2M}\right) m E^{\frac{(M+1)}{2M}} \\ &+ i \sum_{n=1}^{\infty} (-1)^{n+1} \frac{2b_n}{\pi} \cos\left(\frac{\pi}{2M}(2n-1)\right) E^{-\frac{(M+1)}{2M}(2n-1)} - g_{\text{nonpert}}(E) \end{aligned} \quad (5.17)$$

where the coefficients b_n are given in terms of $f(\theta)$ by

$$ib_n = \int_{C_1} (re^\theta)^{2n-1} \log(1 + e^{f(\theta)}) d\theta - \int_{C_2} (re^\theta)^{2n-1} \log(1 + e^{-f(\theta)}) d\theta \quad (5.18)$$

and

$$g_{\text{nonpert}}(E) = \log \left(\frac{1 + e^{-f(\gamma + \frac{\pi i}{2} \frac{|M-1|}{M})}}{1 + e^{f(\gamma - \frac{\pi i}{2} \frac{|M-1|}{M})}} \right). \quad (5.19)$$

(After the expansion has been made, the contours in (5.18) can be shifted back to their original locations without encountering any poles.) The geometrical interpretation of g_{nonpert} will be clearest if the branch of the logarithm in (5.19) is taken in the interval $[-\pi, \pi)$, and this will be assumed from now on; note that this choice has no effect on the quantization condition on the eigenvalues.

For $\frac{1}{2} < M < 1$, the result is instead

$$g(E) \sim 2i\pi(l+\frac{1}{2}) + i \sum_{n=1}^{\infty} (-1)^n \frac{2M c_n}{\pi} \sin(\pi M n) E^{-(M+1)n} + g_{\text{nonpert}}(E) \quad (5.20)$$

with coefficients c_n given by

$$i c_n = \int_{C_1} (r e^\theta)^{2Mn} \log(1 + e^{f(\theta)}) d\theta - \int_{C_2} (r e^\theta)^{2Mn} \log(1 + e^{-f(\theta)}) d\theta \quad (5.21)$$

and $g_{\text{nonpert}}(E)$ is again given by (5.19). Note that g_{nonpert} now contributes with the opposite sign, while the modulus signs in the formula mean that the numerator is always evaluated above the real axis, and the denominator below, if γ is real.

The integrals for the coefficients b_n and c_n are known exactly in terms of the ground state eigenvalues of the local and non-local conserved charges of the zero-mass limit of the sine-Gordon model on a circle [36, 29]. Translating[‡] the results from these papers into the current normalisations,

$$b_n = \frac{\pi^{3/2} (4M+4)^n}{n!} \frac{2n-1}{2n-1} \frac{\Gamma((\frac{1}{2}+\frac{1}{2M})(2n-1))}{\Gamma(\frac{1}{2M}(2n-1))} I_{2n-1}; \quad (5.22)$$

$$c_n = -\frac{2\pi}{M} \frac{2^{2Mn}}{(M+1)^{2n}} \cos(\pi M n) \tilde{H}_n. \quad (5.23)$$

Here, I_{2n-1} and \tilde{H}_n are respectively the ground state eigenvalues of \mathbb{I}_{2n-1} , the n^{th} local conserved charge, and $\tilde{\mathbb{H}}_n$, the n^{th} (dual) nonlocal conserved charge. The precise definitions of these charges can be found in [36, 29, 33] (see also [37, 38]). Explicit expressions for the local charge eigenvalues can be found up to high order; the first three are

$$\begin{aligned} I_1 &= \frac{1}{(4M+4)} \left[\lambda^2 - \frac{M+1}{6} \right], \\ I_3 &= \frac{1}{(4M+4)^2} \left[\lambda^4 - (M+1)\lambda^2 - \frac{(M+1)(4M+3)(M-3)}{60} \right], \\ I_5 &= \frac{1}{(4M+4)^3} \left[\lambda^6 - \frac{5(M+1)}{2}\lambda^4 - \frac{(M+1)(4M^2-23M-23)}{12}\lambda^2 \right. \\ &\quad \left. - \frac{(M+1)(96M^4-340M^3+85M^2+850M+425)}{1512} \right], \end{aligned} \quad (5.24)$$

where $\lambda = l + \frac{1}{2}$. The nonlocal charge eigenvalues are harder to calculate, but the first one is also known in closed form:

$$\tilde{H}_1 = \frac{(M+1)^2 \Gamma(M+1) \Gamma(-2M-1) \Gamma(M+1+\lambda)}{\Gamma(-M) \Gamma(-M+\lambda)}. \quad (5.25)$$

[‡]The dictionary [24, 25] is $\beta^2 = 1/(M+1)$, $p = (2l+1)/(4M+4)$.

Finally, the beyond-all-orders term $g_{\text{nonpert}}(E)$ in (5.17) and (5.20) should be treated, which contains the so-far unknown function $f(\theta)$. We first note that for γ real $f(\gamma - \frac{\pi i}{2} \frac{|M-1|}{M}) = -f^*(\gamma + \frac{\pi i}{2} \frac{|M-1|}{M})$ (the * denoting complex conjugation) and so

$$g_{\text{nonpert}}(E) = 2i \arg \left(1 + e^{-f(\gamma + \frac{\pi i}{2} \frac{|M-1|}{M})} \right). \quad (5.26)$$

Given the branch chosen for the logarithm just after (5.19), the value of the argument in (5.26) lies between $-\pi$ and π . In principle the full asymptotic expansion for f , to be given in the next section, could now be substituted into this formula. However the interesting structure is already seen if the leading behaviour is used, which, from (4.14), is

$$f(\gamma + \frac{\pi i}{2} \frac{|M-1|}{M}) \sim i\pi(l + \frac{1}{2}) - im e^{\frac{\pi i}{2} \frac{|M-1|}{M}} E^{\frac{M+1}{2M}}. \quad (5.27)$$

Hence

$$g_{\text{nonpert}}(E) \sim 2i \arg \left(1 + \rho e^{i\phi} \right) \quad (5.28)$$

where

$$\rho(E) = e^{-m \sin \frac{\pi|M-1|}{2M} E^{\frac{M+1}{2M}}}; \quad (5.29)$$

$$\phi(E) = -\pi(l + \frac{1}{2}) + m \cos \frac{\pi|M-1|}{2M} E^{\frac{M+1}{2M}}. \quad (5.30)$$

The final formula can be given a pictorial interpretation: $g_{\text{nonpert}}(E)$ is approximately equal to $2i \chi(E)$, where $\chi(E)$ the interior angle of the triangle shown in figure 4.

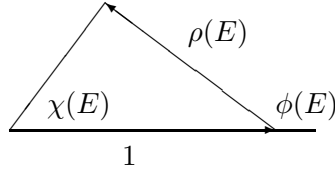


Figure 4: The trigonometry of $g_{\text{nonpert}}(E)$.

Notice that $\rho(E)$ is always less than 1 for $M \neq 1$, and that as E increases with M fixed the point $1 + \rho e^{i\phi}$ executes a diminishing spiral about 1, giving $\chi(E)$ a damped oscillation between $-\pi/2$ and $\pi/2$ which captures the behaviour seen for $M < 1$ in figure 3a above. The nonperturbative nature of $g_{\text{nonpert}}(E)$ is easily seen: $|\chi(E)|$ is bounded by $\frac{\pi}{2}\rho(E)$; and at fixed M , the expansion parameters for the perturbative series parts of (5.17) and (5.20) are $\varepsilon := E^{-\frac{M+1}{2M}}$ and $\eta := E^{-(M+1)}$ respectively, in terms of which $\frac{\pi}{2}\rho$ is equal to either $\frac{\pi}{2} \exp(-m \sin \frac{|M-1|}{M} / \varepsilon)$ or $\frac{\pi}{2} \exp(-m \sin \frac{|M-1|}{M} / \eta^{\frac{1}{2M}})$.

If on the other hand M is taken very close to 1 with E remaining finite, the nonperturbative term plays a key role. In this limit, $\rho(E) \approx 1$ and hence, from figure 4, $\chi(E) \approx \phi(E)/2$, and

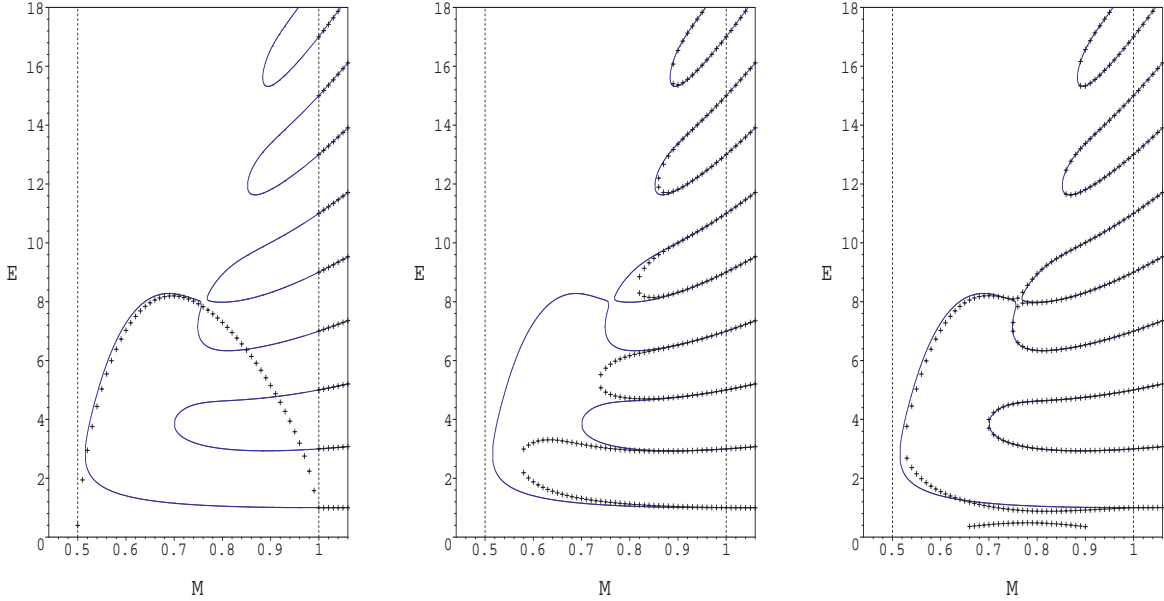
$$g_{\text{nonpert}}(E) \approx -i\pi(l + \frac{1}{2}) + im E^{\frac{M+1}{2M}}. \quad (5.31)$$

This is just the behaviour required if the nonperturbative term is to ‘smooth’ the discontinuous change in the leading asymptotic of $g(E)$ as M passes through 1, seen in equations (5.12) – (5.14) above. The phenomenon is reminiscent of the smoothing of Stokes’s discontinuities discussed in [40]. Strictly speaking, since χ remains between $-\pi/2$ and $\pi/2$ the limit of

$g_{\text{nonpert}}(E)/i$ as $M \rightarrow 1$ is a sawtooth function obtained by returning the imaginary part of the RHS of (5.31), modulo 2π , to the interval $[-\pi, \pi]$. This has an important effect on the counting of eigenvalues. Consider for example the limit $M \rightarrow 1^-$ at fixed E : since the coefficients in series part of (5.20) are all of order $\epsilon = 2 - 2M$, the limiting form of $g(E)$ is

$$g(E)\Big|_{M=1^-} = 2\pi i(l + \frac{1}{2}) - \pi i \left[l + \frac{1}{2} - \frac{1}{2}E \right]_{[-1,1]} \quad (5.32)$$

where the subscript on the last term indicates that it should be returned, modulo 2, to the interval $[-1, 1]$ – so $[x]_{[-1,1]} := (x+1) \bmod 2 - 1$. Since g is continuous for all $M < 1$, its $M \rightarrow 1^-$ limit has segments of infinite gradient at the points $l + \frac{1}{2} - \frac{1}{2}E = (2k+1)$ where the corresponding sawtooth function would have a discontinuity. The quantisation condition $g(E) = (2n+1)\pi i$ is therefore *always* satisfied at these values of E , in addition to the points $l + \frac{1}{2} + \frac{1}{2}E = (2k+1)$ which would have been found even before taking the sawtooth effect into account. Taken together, these points match the full spectrum of the PT-symmetric simple harmonic oscillator, discussed from another point of view just after equation (5.15) above; the crucial role played by the nonperturbative term in this process is interesting.



5a: Perturbative term

5b: Nonperturbative term

5c: Both terms

Figure 5: Different approximation schemes for the energy levels (small crosses) compared with the exact levels (continuous lines), for $l = -0.001$.

More generally, for $M < 1$ and $l \neq 0$ the nonperturbative term explains the infinite sequence of merging levels high in the spectrum, while perturbative term is responsible for the single level joined to the ground state which moves upwards as $l \rightarrow 0$. To understand the reversed connectivity below this level, both effects must be incorporated simultaneously. Figure 5 illustrates this by comparing the exact energy levels, computed using the full nonlinear integral equation, with the levels obtained by combining the leading asymptotic of $g(E)$, (5.12) - (5.14), with either a) the first perturbative correction, or b) the leading approximation to the nonperturbative correction, or c) both. (Note that the lowest group of crosses in figure 5c at intermediate values of M is spurious, being caused by the over-large contribution of the perturbative correction at such small values of E .)

Explicitly, the crosses on figure 5c mark points at which $g_{\text{approx}}(E) = (2k+1)\pi i$, where

$$g_{\text{approx}}(E) = \begin{cases} 2im \sin(\frac{\pi}{2M}) E^{\frac{(M+1)}{2M}} + \frac{i\pi^{3/2} (6(l+\frac{1}{2})^2 - M - 1)}{3\Gamma(\frac{1}{2M})\Gamma(\frac{1}{2} - \frac{1}{2M})} E^{-\frac{(M+1)}{2M}} - g_{\text{nonpert}}(E) & (M > 1); \\ 2i\pi(l+\frac{1}{2}) + \frac{i\pi^{3/2} \Gamma(M+\frac{3}{2}+l)}{\Gamma(M+\frac{3}{2})\Gamma(-M)\Gamma(-M+\frac{1}{2}+l)} E^{-(M+1)} + g_{\text{nonpert}}(E) & (M < 1), \end{cases} \quad (5.33)$$

with $g_{\text{nonpert}}(E)$ given by the leading approximation (5.28), and m by (4.15). For figure 5a, only the first and second terms on each RHS were used for g_{approx} ; for figure 5b, only the first and third.

Even for the low-lying levels, the combined approximation does very well. Figure 6 shows a more stringent test by zooming in on the first three level-mergings; again, the match is very good. The errors are greatest in figure 6b, near to the second merging. This is not surprising since the recombination of levels occurring there makes the locations of the eigenvalues particularly sensitive to errors in the value of $g(E)$. These errors become smaller for recombinations higher up the spectrum.

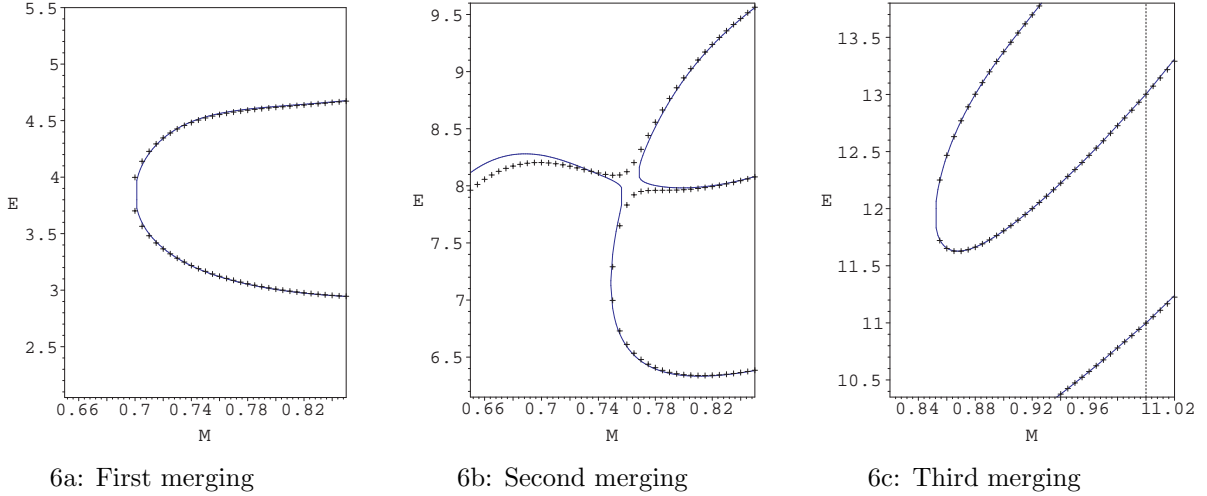


Figure 6: The perturbative-plus-nonperturbative approximation for $l = -0.001$ (small crosses) compared with the exact levels (continuous lines) near the first three level mergings shown on figure 5c.

To analyse the level-mergings for $M < 1$ in more detail, we take $\epsilon = 2M - 2$ small and negative, and E fixed but large. Then the limiting form of the quantisation condition arising from (5.33) can be written as

$$\chi(E) = \pi k - \pi l + \frac{\pi}{3} (l + \frac{3}{2})(l^2 - \frac{1}{4}) |\epsilon| E^{-2} \quad (5.34)$$

where $k \in \mathbb{Z}$, $\chi(E) \equiv \frac{1}{2i} g_{\text{nonpert}}(E)$ is the angle shown on figure 4, and, to the same approximation, the other quantities on the figure are

$$\rho(E) = e^{-\frac{\pi^2}{8} |\epsilon| E}; \quad (5.35)$$

$$\phi(E) = -\pi(l + \frac{1}{2}) + \frac{\pi}{2} E + \frac{\pi}{8} |\epsilon| E \ln(E). \quad (5.36)$$

Since $\chi(E)$ is always between $-\pi/2$ and $\pi/2$, all solutions to (5.34) for l small have $k = 0$. If l is nonzero, then sufficiently high in the spectrum the final term on the RHS of (5.34) becomes

insignificant and the condition reduces to $\chi(E) = -\pi l$. This is illustrated in figure 7: given that ϵ is small, ρ behaves as a slow mode in E , and ϕ as a fast mode, and so the point $1 + \rho e^{i\phi}$ moves around the circle of approximately-constant radius ρ , this radius slowly decreasing as E increases. Eigenvalues occur when this point crosses the ray from the origin with argument $-\pi l$. Two such rays are shown on the figure: one, the upper dashed line, is for $l < 0$, and the other, the lower dashed line, is for $l > 0$.

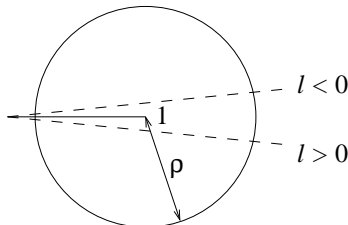


Figure 7: The approximate quantisation condition for $l \neq 0$.

If ρ becomes too small, the circle and the ray cease to intersect and so the eigenvalue condition can never be met, no matter what (real) value is taken by the fast mode ϕ . This means that the eigenvalues have merged to become complex. The critical value of ρ at which this first occurs is $|\sin(\pi l)|$; hence, the merging of eigenvalues occurs asymptotically along the curve

$$E = -\frac{8 \ln |\sin(\pi l)|}{\pi^2 |\epsilon|} . \quad (5.37)$$

The curved dotted lines on figures 1a, 1b and 1d allow (5.37) to be compared with the behaviour of the exact levels.

We can also predict which eigenvalues pair off, by thinking about the fast mode ϕ . If E is kept approximately fixed and $|\epsilon|$ is increased (since $\epsilon < 0$, this corresponds to decreasing M), then from (5.35) ρ decreases while ϕ is unchanged. This makes it easy to see that it is pairs of eigenvalues associated with neighbouring crossings of the ray $\arg(z) = -\pi l$ on the *same* side of the real axis which merge. Now as E increases from zero, the phase ϕ increases from $-\pi/2 - \pi l$, meaning that the point $1 + \rho e^{i\phi}$ starts below the real axis. If $l < 0$, it first crosses into the upper half plane before encountering the ray $\arg(z) = -\pi l$, which it then does twice before crossing the real axis again. Hence the lowest level is paired with the second level, the third with the fourth and so on. If on the other hand $l > 0$, then starting again from $E = 0$ the point $1 + \rho e^{i\phi}$ encounters the ray $\arg(z) = -\pi l$ *once*, below the real axis, then moves anticlockwise through the upper half z -plane before the next two crossings of the ray, both below the real axis, occur. Hence the connectivity of the levels is reversed, with the second and third, fourth and fifth, and so on, levels pairing off. This is exactly as observed in our earlier numerical work, now predicted analytically.

Strictly speaking, we have just found the connectivities that the levels would have were they quantised by the nonperturbative term alone, since we discarded the final term on the RHS of (5.34) before commencing the analysis. However, if E is taken large enough before ϵ is sent to zero, then this term dominates and so our argument also predicts the connectivity of the true level-mergings, high up the spectrum. Lower down, the behaviour of the true levels may differ from that of the nonperturbative-only approximation, as can be seen by comparing figures 5b and 5c. This corresponds to the recombination of levels, and simple estimate of where it occurs can be obtained by finding the intersection of the curve (5.37) with the curve $\frac{\pi}{3}(l + \frac{3}{2})(l^2 - \frac{1}{4})|\epsilon|E^{-2} = \pi l$, which approximates the energy level found by quantizing according

to the perturbative term alone, shown for $l = -0.001$ in figure 5a. For small $l < 0$, this yields

$$E_{\text{recomb}}(l) = \left(\frac{\ln |\pi l|}{\pi^2 l} \right)^{1/3}. \quad (5.38)$$

For $l = -0.001$, $E_{\text{recomb}} \approx 8.36$, which matches well the behaviour shown in figures 1c and 5.

It remains to treat the marginal case, $l = 0$. This is much more delicate. Easiest to discuss is the connectivity of the levels. The last term in (5.34) functions much as the term $-\pi l$ did before from the point of view of the fast mode ϕ ; given its sign, this means that the connectivity of levels for $l = 0$ is the same as that for $l > 0$, which is indeed what was observed numerically. (A similar argument explains why the connectivity is reversed below $E = E_{\text{recomb}}$ for $l < 0$.) To estimate where the level merging occurs, note that the critical value of ρ is now $\sin(\frac{\pi}{8}|\epsilon|E^{-2})$. For large E and small ϵ we must therefore solve

$$e^{-\frac{\pi^2}{8}|\epsilon|E} = \frac{\pi}{8}|\epsilon|E^{-2} \quad (5.39)$$

to find the critical value of E . The solution can be expressed in terms of the Lambert W function $W(x)$, which is defined to satisfy $W(x)e^{W(x)} = x$. (More information on this function can be found in [41]; it is related to the tree function $T(x)$ by $W(x) = -T(-x)$.) Explicitly,

$$E = -\frac{16}{\pi^2|\epsilon|} W_{-1} \left(-\frac{\pi^{5/2}|\epsilon|^{3/2}}{32\sqrt{2}} \right) \quad (5.40)$$

where the subscript -1 selects the relevant branch of the W function (see [41]). Now using the asymptotic $T_{-1}(x) = -W_{-1}(-x) \sim \ln(x^{-1}) + \ln(\ln(x^{-1}))$ for $x \rightarrow 0^+$, the curve (5.37), which diverges as $l \rightarrow 0$, should be replaced by

$$E \sim \frac{16}{\pi^2|\epsilon|} \left[\ln \left(\frac{32\sqrt{2}}{\pi^{5/2}|\epsilon|^{3/2}} \right) + \ln \ln \left(\frac{32\sqrt{2}}{\pi^{5/2}|\epsilon|^{3/2}} \right) \right]. \quad (5.41)$$

This corrects the result of [5], equation (3.6) above, and shows that while the two-by-two truncation used in that paper gives a qualitative understanding of the situation, is too crude to capture precise asymptotics. However, even with the second logarithm included in (5.41), or using the W function directly, the approach of the level-mergings to their asymptotic locations for $l = 0$ is much slower than that found for nonzero values of l . The dotted line on figure 1c compares (5.40) with the exact levels, obtained by solving the nonlinear integral equation.

6 Asymptotics for the radial problem

The approach of the previous sections can also be applied to the more-standard radial problem (4.1). The analysis is very similar to that already given, though simpler because the subtleties of the second determination do not apply.

The large- θ expansion of the first-determination kernel (4.17) is

$$\varphi(\theta) \sim -\sum_{n=1}^{\infty} \frac{1}{\pi} \cot\left(\frac{\pi}{2M}(2n-1)\right) e^{-(2n-1)\theta} + \sum_{n=1}^{\infty} \frac{M}{\pi} \tan(\pi Mn) e^{-2Mn\theta} \quad (6.1)$$

and so for large real θ ,

$$f(E) \sim i\pi(l+\frac{1}{2}) - i \sum_{n=0}^{\infty} \frac{b_n}{\pi} \cot(\frac{\pi}{2M}(2n-1)) E^{-\frac{(M+1)(2n-1)}{2M}} + i \sum_{n=1}^{\infty} \frac{Mc_n}{\pi} \tan(\pi Mn) E^{-(M+1)n}, \quad (6.2)$$

where b_n , c_n and m are as before, and we defined $b_0 = -\pi \tan(\frac{\pi}{2M})m$ so as to absorb the exponentially-growing part of the asymptotic into the first series. The condition for E to be an eigenvalue of the radial problem can be written as

$$f(E) = -(2k+1)\pi i, \quad k \in \mathbb{Z} \quad (6.3)$$

Written directly in terms of the conserved charges, and setting $I_{-1} := 1$, the expansion coefficients of f are

$$-i \frac{b_n}{\pi} \cot(\frac{\pi}{2M}(2n-1)) = i(-1)^n \frac{\sqrt{\pi} \Gamma(1 - \frac{(2n-1)}{2M})}{\Gamma(\frac{3}{2} - n - \frac{(2n-1)}{2M})} \frac{(4M+4)^n}{(2n-1)n!} I_{2n-1}; \quad (6.4)$$

$$i \frac{Mc_n}{\pi} \tan(\pi Mn) = -2i \sin(\pi Mn) \frac{2^{2Mn}}{(M+1)^{2n}} \tilde{H}_n. \quad (6.5)$$

Notice that (6.2) is a double series, unlike the single series (5.17) and (5.20) found for the lateral problems, and that its form does not change as we move between the attractive ($M > 1$) and the repulsive ($M < 1$) regimes. For $M < 2$ the steepest-descent contour lies inside the first determination, at least for large E , and so, unlike for the PT-symmetric problem discussed above, there is no need to add a non-perturbative term. The double series could also have been recovered directly from the asymptotics of $Q(\theta)$ found in [29], given the ODE/IM correspondence. Taking suitable care about the branch choices, the same applies to the series parts of the expansions for the lateral problems obtained in the last section, but the beyond all orders contributions would have been missed.

For the radial problem, the WKB method should work for all values of M , and it is natural to try to recover the asymptotics from a direct analysis of the differential equation. In the rest of this section we show how the contributions to (6.2) from local conserved quantities can be found using an all-orders WKB approximation, and give some hints as to the origins of the nonlocal parts. Even for the local part of the discussion, there are some interesting features, as the application of the WKB technique to radial problems is tricky [42, 43, 44].

A WKB treatment of the radial problem might begin by writing (4.1) as

$$\left[-\frac{d^2}{dx^2} + \overline{Q}(x) \right] y = 0, \quad \overline{Q}(x) = x^{2M} - E + \frac{l(l+1)}{x^2}. \quad (6.6)$$

For l and E positive, $\overline{Q}(x)$ has two simple zeroes on the positive x axis: one, x_0 , near $x = 0$ and the other, x_1 , near $x = E^{1/2M}$. The leading WKB quantisation condition would then be $2 \int_{x_0}^{x_1} \sqrt{-\overline{Q}(x)} dx = (2k+1)\pi$, $k \in \mathbb{Z}$. However, this does not give good results. The reason, first stressed by Langer [42], is that the WKB approximation derived from (6.6) breaks down near $x = 0$. Instead, Langer suggested making a preliminary change of variable

$$x = e^z \quad (6.7)$$

and gauge transformation

$$y(x) = e^{z/2}\psi(z) \quad (6.8)$$

so that (6.6) becomes

$$\left[-\frac{d^2}{dz^2} + \tilde{Q}(z) \right] \psi = 0 \quad , \quad \tilde{Q}(z) = e^{(2M+2)z} - Ee^{2z} + (l+1/2)^2. \quad (6.9)$$

The quantisation condition for the modified problem is

$$2 \int_{z_0}^{z_1} \sqrt{-\tilde{Q}(z)} dz = (2k+1)\pi, \quad k \in \mathbb{Z}, \quad (6.10)$$

which, changing the variable back to $\ln z = x$, amounts to the trading of $l(l+1)$ with $\lambda^2 = (l+1/2)^2$ in the original potential. This is sometimes called the Langer modification, and it allows the energy levels of the radial harmonic oscillator and the radial Coulomb potential to be recovered exactly. However, away from these points, the generalisation to incorporate higher-order WKB corrections is difficult. In particular, the leading l -dependence in (6.2), namely the term $i\pi(l+\frac{1}{2})$, only emerges once an all-orders resummation has been performed [44].

The problem is that l and E are badly tangled up in formulae such as (6.10). To get round this, we take the Langer-transformed equation (6.9) and change variable $z \rightarrow \gamma z$. Transforming back to the variable x , using (6.7) and (6.8) in reverse, we find

$$\left[-\frac{d^2}{dx^2} + \gamma^2 x^{(2M+2)\gamma-2} - E\gamma^2 x^{2\gamma-2} + \frac{\tilde{l}(\tilde{l}+1)}{x^2} \right] y = 0 \quad (6.11)$$

where

$$\tilde{l} = \gamma\lambda - 1/2. \quad (6.12)$$

If $\gamma = 1/(2\lambda)$ then $\tilde{l} = 0$, and, changing variable to $t = E^{-\lambda/M}x$, (6.11) simplifies to

$$\left[-\varepsilon^2 \frac{d^2}{dt^2} + Q(t) \right] y(t) = 0 \quad (6.13)$$

where

$$Q(t) = \frac{1}{4\lambda^2} t^{1/\lambda-2} (t^{M/\lambda} - 1), \quad \varepsilon = E^{-(M+1)/2M}. \quad (6.14)$$

A key feature of this equation is that the E -dependence, contained in ε , has been factored out of the transformed potential $Q(t)$. In fact, ε takes the role of the variable which organises the whole higher-order WKB series, in eq. (6.24) below. This means that a systematic WKB treatment of the transformed equation should yield the asymptotic behaviour of the energy levels as $E \rightarrow \infty$ at fixed M and l , which is just what we want. The contrast with (6.9) accounts for the difficulties encountered when trying to work directly with the Langer-transformed equation. The simplification has a price, though: for $l \neq 0$ the turning point which had been near the origin is replaced by a singularity of order $1/\lambda - 2$ exactly at $x = 0$. This requires special treatment, which we illustrate by calculating the leading correction explicitly by asymptotic matching.

To build a solution which to leading ('physical optics') asymptotic approximation solves the transformed eigenvalue problem, the t axis can be split into four regions, defined for

$\varepsilon \rightarrow 0^+$ as follows[§]:

$$\begin{aligned}
\text{Region I} & : t > 1, |t-1| \gg \varepsilon^{2/3} \\
\text{Region II} & : |t-1| \ll 1 \\
\text{Region III} & : 1 > t > 0, |t| \gg \varepsilon^{2\lambda}, |1-t| \gg \varepsilon^{2/3} \\
\text{Region IV} & : t > 0, |t| \ll 1
\end{aligned} \tag{6.15}$$

In regions I and III, the physical optics approximation is good, while regions II and IV need separate treatment. In region I, the decaying WKB solution is

$$y_I(t) = \frac{1}{[Q(t)]^{1/4}} \exp \left[-\frac{1}{\varepsilon} \int_1^t \sqrt{Q(u)} du \right]. \tag{6.16}$$

This can be continued through region II, which contains the simple turning point at $t = 1$, using an Airy function in the standard way [45], to find $y(t) \sim y_{\text{III}}(t)$ in region III, where

$$y_{\text{III}}(t) = \frac{2}{[-Q(t)]^{1/4}} \cos \left[-\frac{1}{\varepsilon} \int_t^1 \sqrt{-Q(u)} du + \frac{\pi}{4} \right]. \tag{6.17}$$

Taking t near zero, but still in region III, this behaves as

$$\begin{aligned}
y_{\text{III}}(t) & = \frac{2}{[-Q(t)]^{1/4}} \cos \left[-\frac{1}{\varepsilon} \int_0^1 \sqrt{-Q(u)} du + \frac{1}{\varepsilon} \int_0^t \sqrt{-Q(u)} du + \frac{\pi}{4} \right] \\
& \sim 2\sqrt{2\lambda} t^{\frac{1}{2} - \frac{1}{4\lambda}} \cos \left[-\frac{1}{\varepsilon} \int_0^1 \sqrt{-Q(u)} du + \frac{1}{\varepsilon} t^{\frac{1}{2\lambda}} + \frac{\pi}{4} \right].
\end{aligned} \tag{6.18}$$

This solution breaks down as $t \rightarrow 0$, and must be matched to a solution of the approximate ODE in region IV, which is

$$\left[-\frac{d^2}{dt^2} - \frac{1}{4\lambda^2 \varepsilon^2} t^{\frac{1}{\lambda} - 2} \right] y(t) = 0 \tag{6.19}$$

Imposing $y \rightarrow 0$ as $t \rightarrow 0$, the appropriate solution is

$$y_{\text{IV}}(t) = \beta \sqrt{t} J_\lambda \left(\frac{1}{\varepsilon} t^{\frac{1}{2\lambda}} \right), \tag{6.20}$$

where J_λ is a Bessel function, and β a so-far arbitrary normalisation constant. (The behaviour as $\frac{1}{\varepsilon} t^{\frac{1}{2\lambda}} \rightarrow 0$ is $y_{\text{IV}}(t) \sim \beta t (2\varepsilon)^{-\lambda} / \Gamma(\lambda+1)$, as follows from the $\xi \rightarrow 0$ asymptotic $J_\lambda(\xi) \sim (\xi/2)^\lambda / \Gamma(\lambda+1)$.) The large- ξ formula $J_\lambda(\xi) \sim \sqrt{\frac{2}{\pi\xi}} \cos \left[\xi - \frac{\lambda}{2}\pi - \frac{\pi}{4} \right]$ then implies

$$y_{\text{IV}}(t) \sim \beta \sqrt{\frac{2\varepsilon}{\pi}} t^{\frac{1}{2} - \frac{1}{4\lambda}} \cos \left(\frac{1}{\varepsilon} t^{\frac{1}{2\lambda}} - \frac{\lambda\pi}{2} - \frac{\pi}{4} \right) \quad \text{for } t \gg \varepsilon^{2\lambda}. \tag{6.21}$$

For E to be an eigenvalue, this should match the small- t form of $y_{\text{III}}(t)$ given by (6.18). This requires

$$\frac{1}{\varepsilon} \int_0^1 \sqrt{-Q(u)} du = k\pi + \frac{\lambda\pi}{2} + \frac{\pi}{2}, \quad \beta = 2\sqrt{\frac{\pi\lambda}{\varepsilon}} (-1)^k, \quad k \in \mathbb{Z}. \tag{6.22}$$

[§]As in [45], $a \ll b$ ($\varepsilon \rightarrow 0^+$) \leftrightarrow $a/b \rightarrow 0$ as $\varepsilon \rightarrow 0^+$

Restoring the original variables and substituting $w = u^{\frac{M}{\lambda}}$ results in a beta-function integral and the quantisation condition

$$\frac{1}{M} B\left(\frac{1}{2M}, \frac{3}{2}\right) E^{\frac{M+1}{2M}} = (2k + l + \frac{3}{2})\pi, \quad k \in \mathbb{Z}. \quad (6.23)$$

Using (4.16), the condition implied by (6.2) is recovered to next-to-leading order[¶]. Notice that the full l -dependence has been recovered directly, without any need for resummation.

Encouraged by this result, it is natural to see how much more of the asymptotic expansion found using the ODE/IM correspondence can be recovered by incorporating higher-order WKB corrections. Suppose that (6.13) has a solution of the form

$$y(t) = \exp\left[\frac{1}{\varepsilon} \sum_{n=0}^{\infty} \varepsilon^n S_n(t)\right]. \quad (6.24)$$

For (6.13) to be satisfied order-by-order in ε , the derivatives $S'_n(t)$ must obey the following recursion relations:

$$S'_0(t) = -\sqrt{Q(t)}, \quad 2S'_0 S'_n + \sum_{j=1}^{n-1} S'_j S'_{n-j} + S''_{n-1} = 0 \quad (n \geq 1). \quad (6.25)$$

The first few terms of the solution are

$$\begin{aligned} S'_0 &= -\sqrt{Q}, \\ S'_1 &= -\frac{Q'}{4Q}, \\ S'_2 &= -\frac{1}{48} \left(\frac{Q''}{Q^{3/2}} + 5 \frac{d}{dz} \left[\frac{Q'}{Q^{3/2}} \right] \right), \\ S'_3 &= -\frac{Q''}{16Q^2} + \frac{5(Q')^2}{64Q^3} = \frac{d}{dz} \left[\frac{5(Q')^2}{64Q^3} - \frac{Q''}{16Q^2} \right], \end{aligned} \quad (6.26)$$

Keeping just S_0 and S_1 constitutes the physical optics approximation employed above; further terms are very easily obtained using, for example, Mathematica. Near to zeros of $Q(t)$ – the so-called turning points – the approximation breaks down and further work is needed to find the connection formulae for the continuation of WKB-like solutions of given order from one region of non-vanishing Q to another, just as was done above. Solutions found by continuation away from the two boundary conditions must then be matched to find the condition for Q to be such that the differential equation has an acceptable solution. This quickly becomes quite complicated, as exemplified by the calculations in section 10.7 of [45].

In cases where Q is entire with just a pair of well-separated simple zeros on the real axis, Dunham [46] found a remarkably simple formulation of the final condition, valid to all orders:

$$\frac{1}{i} \oint \sum_{n=0}^{\infty} \varepsilon^{n-1} S'_n(z) dz = 2k\pi, \quad k \in \mathbb{Z} \quad (6.27)$$

[¶]Following Langer [42], the same result can also be obtained starting from the approximation $y(t) \sim [-Q(t)]^{-1/4} \xi^{1/2} (\alpha J_{-\lambda}(\xi) + \beta J_{\lambda}(\xi))$ in the region $t \approx 0$, with $\xi = \int_0^t \sqrt{-Q(u)} du$, and the boundary condition at $t = 0$ requiring $\alpha = 0$.

where the contour encloses the two turning points; it closes because for such a Q all of the functions S'_n derived from (6.25) are either entire, or else have a pair of square root branch points which can be connected by a branch cut along the real axis. Notice that the contour can be taken to lie far from the two turning points, where the WKB series breaks down, and so there is no need to worry about connection formulae. All of the terms S'_{2n+1} , $n \geq 1$, turn out to be total derivatives and can therefore be discarded, while $\frac{1}{2i}S'_1 = -\frac{1}{8i}Q'/Q$ and contributes a simple factor of $\pi/2$ when integrated round the two zeros of Q , irrespective of any other details. Dunham's condition is therefore

$$\frac{1}{i} \oint \sum_{n=0}^{\infty} \varepsilon^{2n-1} S'_{2n}(z) dz = (2k+1)\pi, \quad k \in \mathbb{Z}. \quad (6.28)$$

However, this method is only directly relevant to the current problem if the angular momentum is zero, and M is an integer. Extensive discussions of these cases can be found in [47], and it is straightforwardly checked that the results found there match the expansion we obtained above using the ODE/IM correspondence. Note that for $M \in \mathbb{Z}$ there are no 'nonlocal' contributions to the asymptotic (6.2), so the WKB series gives the complete answer.

For more general cases there is only one simple turning point, the other being replaced by the singularity at $z = 0$, and the analysis just given does not apply. Nevertheless, the E -dependence of (6.2) together with the match with the results of [47] at special points suggests that the contributions to the asymptotic related to the *local* integrals of motion might still be obtained from a WKB series of the form (6.28), suitably treated. The main difficulty is the fractional singularity at $z = 0$, which prevents the contour in Dunham's condition from closing. However, away from regions about $z = 0$ and $z = 1$ which are vanishingly small as $\varepsilon \rightarrow 0$, the all-orders WKB solution provides a good approximation to the true wavefunction. As an *ad hoc* measure, we replace the closed Dunham contour in (6.27) by a contour \mathcal{C} which starts just below the origin, passes once round the turning point at $z = 1$, and returns to a point just above the origin. Since all of the terms S'_{2n+1} , $n \geq 1$, are total derivatives of functions which are single-valued around $z = 1$, they again make no contribution even though the contour is no longer closed. Therefore we replace Dunham's condition (6.28) by

$$\frac{1}{i} \int_{\mathcal{C}} \sum_{n=0}^{\infty} \varepsilon^{2n-1} S'_{2n}(z) dz = (2k + \frac{1}{2} + 2\delta)\pi, \quad k \in \mathbb{Z} \quad (6.29)$$

where S'_{2n} is obtained from (6.25) using the Q given by (6.14), and the factor 2δ allows for a possible phase-shift caused by the singularity at the origin. From the initial asymptotic matching calculation, the leading (constant) part of 2δ is $\lambda + 1/2$, but further E -dependent corrections can be expected – we shall return to this issue below.

For concrete calculations, it is convenient to collapse the contour \mathcal{C} onto real axis, and the square root singularities of the integrands at $z = 1$ then allow each integral to be replaced by $2 \int_0^1 S'_{2n}(t) dt$. A difficulty with this procedure is that the divergences in the WKB series at $z = 1$ are no longer avoided. We remedied this by multiplying each integrand $S'_{2n}(t)$ by $(t^{M/\lambda} - 1)^\kappa$ to force convergence, doing the definite integrals – still possible in closed form – and then setting $\kappa = 0$ at the end. It is a simple matter to mechanise the calculation with a few lines of Mathematica code, and, using (6.4) in reverse, the values of the local charges I_1 , I_3 and I_5 given in (5.24) are easily reobtained; we also reproduced the formulae for I_7 and I_9 quoted in [36, 39], though these are rather too lengthy to be worth repeating here. It is interesting that the values of the conserved charges in the quantum field theory

can be recovered by such relatively-straightforward manipulations of the ordinary differential equation.

Finally, the phase shift δ should be analysed. We claim that this is related to the part of the asymptotic due to non-local conserved charges. To see why, focus on the behaviour near the origin by changing variables one more time in (6.13), to $u := \varepsilon^{-2\lambda}t$. The equation becomes

$$\left[-\frac{d^2}{du^2} - \frac{1}{4\lambda^2} u^{1/\lambda-2} + \frac{1}{4\lambda^2} \varepsilon^{2M} u^{(M+1)/\lambda-2}\right] y(u) = 0. \quad (6.30)$$

Treating the final term as a perturbation results in a series of corrections to $y(u)$ as powers of $\varepsilon^{2M} = E^{-(M+1)}$. Comparing with (6.2), this is exactly the structure of the second series of terms emerging from the ODE/IM correspondence, encoding the values of the non-local conserved charges in the integrable model.

In more detail, the perturbative treatment begins with the unperturbed equation

$$\left[-\frac{d^2}{du^2} - \frac{1}{4\lambda^2} u^{1/\lambda-2}\right] y(u) = 0. \quad (6.31)$$

Two independent solutions j and n are

$$j(u) = \sqrt{u} J_\lambda(u^{1/2\lambda}) \quad , \quad n(u) = \sqrt{u} Y_\lambda(u^{1/2\lambda}). \quad (6.32)$$

Their Wronskian is $W[j, n] := j(u)n'(u) - j'(u)n(u) = \frac{1}{\pi\lambda}$ and using this fact it can be checked (as in for example [48, 49]) that, with the boundary condition $y(u) \sim j(u)$ as $u \rightarrow 0$, the full differential equation (6.30) is equivalent to the integral equation

$$y(u) = j(u) + \varepsilon^{2M} \int_0^u G(u|s) v(s) y(s) ds \quad (6.33)$$

where

$$G(u|s) = \pi\lambda [n(u)j(s) - n(s)j(u)] \quad (6.34)$$

and

$$v(u) = \frac{1}{4\lambda^2} u^{(M+1)/\lambda-2}. \quad (6.35)$$

Formally, (6.33) can be solved by iteration. The zeroth order result is proportional to $y_{IV}(t)$, defined in (6.20); later terms give the Born series for the problem.

To extract the corrected phase shift, the RHS of (6.33) can be rewritten as

$$y(u) = j(u) \left[1 - \varepsilon^{2M} \int_0^u \pi\lambda n(s) v(s) y(s) ds\right] + n(u) \varepsilon^{2M} \int_0^u \pi\lambda j(s) v(s) y(s) ds. \quad (6.36)$$

The large- u asymptotics

$$j(u) \sim \sqrt{\frac{2}{\pi}} u^{\frac{1}{2} - \frac{1}{4\lambda}} \cos\left(u^{\frac{1}{2\lambda}} - \frac{\lambda\pi}{2} - \frac{\pi}{4}\right), \quad n(u) \sim \sqrt{\frac{2}{\pi}} u^{\frac{1}{2} - \frac{1}{4\lambda}} \sin\left(u^{\frac{1}{2\lambda}} - \frac{\lambda\pi}{2} - \frac{\pi}{4}\right) \quad (6.37)$$

then yield

$$y(u) \sim \sqrt{\frac{2}{\pi}} u^{\frac{1}{2} - \frac{1}{4\lambda}} A(u) \cos\left(u^{\frac{1}{2\lambda}} - \pi\delta\right) \quad (6.38)$$

where

$$\tan\left(\pi\delta - \frac{\lambda\pi}{2} - \frac{\pi}{4}\right) = \varepsilon^{2M} \int_0^u \pi\lambda j(s) v(s) y(s) ds \Big/ \left[1 - \varepsilon^{2M} \int_0^u \pi\lambda n(s) v(s) y(s) ds\right]. \quad (6.39)$$

In problems with localised perturbing potentials, the integrals in (6.39), and also the function $A(u)$ in (6.38), tend to finite limits as $u \rightarrow \infty$. Replacing $y(s)$ on the RHS of (6.39) by the Born series generated by (6.33) then gives the perturbative expansion of the phase shift. This must be treated with some caution here, since the perturbing potential (6.35) in general grows at infinity. However, at least at first order – the so-called Born approximation – it is possible to extract sensible results.

The leading behaviour of (6.33) is simply $y(u) \approx j(u)$. At this order there is no contribution from the denominator in (6.39), and so the once-corrected phase shift is, formally,

$$\begin{aligned} \delta &= \frac{\lambda}{2} + \frac{1}{4} + \varepsilon^{2M} \int_0^\infty \lambda v(s) j(s)^2 ds + \dots \\ &= \frac{\lambda}{2} + \frac{1}{4} + \frac{1}{2} E^{-(M+1)} \int_0^\infty x^{2M+1} J_\lambda(x)^2 dx + \dots \end{aligned} \quad (6.40)$$

The last integral converges for $M+1+\lambda > 0$, $2M+1 < 0$, and in this region its value (found using Mathematica, or, for example, page 237 of [50]) is

$$\int_0^\infty x^{2M+1} J_\lambda(x)^2 dx = \frac{\Gamma(-M-\frac{1}{2})\Gamma(M+1+\lambda)}{\sqrt{2\pi}\Gamma(-M)\Gamma(-M+\lambda)}. \quad (6.41)$$

Using (6.5), this reproduces the value of \tilde{H}_1 given by (5.25) above.

The agreement with previous results provides some retrospective justification for our procedure, though we cannot rule out the appearance of subtleties at higher orders. Clearly, a more rigorous and systematic treatment would be desirable, especially given the difficulties in evaluating the eigenvalues of the nonlocal charges directly within the quantum field theory. However, we shall leave further investigation of this point for future work.

7 Conclusions

We have given a concrete application of the ODE/IM correspondence by showing how it can be used to obtain an analytic understanding of the level mergings in the model introduced by Bender and Boettcher, one of the longest-studied examples of \mathcal{PT} symmetric quantum mechanics. The subtle mixture of perturbative and nonperturbative effects contributing to the recombination of levels in the generalisation of the model to include a centrifugal term is particularly striking, and shows once again the surprising richness of \mathcal{PT} symmetry as a source of interesting problems in mathematical physics.

There are many questions left unanswered by our work, and we finish by mentioning just a few potentially interesting directions for further investigations.

First of all, the origin of the perturbative and nonperturbative terms for $M < 1$ should be understood through more standard differential equation techniques. For the nonperturbative term responsible for the level-mergings, we expect that the complex WKB method will play a role, as in [9]. This could enable the study of models not treatable with the (less conventional) methods described in this paper. An alternative strategy for systems with potentials of the form $P(x)/x^2$ with $P(x)$ a polynomial would be to use the set of functional relations (the fusion hierarchy) satisfied by the spectral determinant $T(E)$, and this could also be explored.

Our discussion of the nonperturbative term was restricted to $M \approx 1$; as mentioned above, when M goes beyond $1/2$ or 2 , the pole responsible for this term no longer crosses the steepest-descent contour and the asymptotic changes. This effect turns out to be most marked near

to $M = 1/2$ for $l = 0$, and in this region some further smoothing is needed before a good approximation for the energy levels can be obtained from the integral equation. Relevant techniques for analogous problems have been developed in [51, 52], but we have yet to apply them to the current situation. It would be interesting to see whether the delicate asymptotic for the diverging ground state energy calculated in [1, 5] could be recovered by such methods.

The perturbative parts of the expansions for both the radial and the lateral problems are especially interesting for the ODE/IM correspondence, since they encode the values of conserved charges in the integrable quantum field theories. Our discussion of the relationship between the Born series and the nonlocal conserved charges at the end of section 6 was rather preliminary, and it would be nice to make the analysis fully rigorous and to push it to higher orders. In this respect, the sophisticated calculations of spectral zeta functions of Chudnovsky, Chudnovsky and Voros [53] are likely to be relevant. The relationship between the local conserved charges and the WKB series is much clearer, but still needs to be understood on a more profound level. On the ODE side, efficient techniques have been developed for the evaluation of higher-order WKB contributions (see for example [54]), and there now seems to be scope to apply these methods to the study of integrable models.

Finally, it would be worthwhile to extend these considerations to other integrable models, and other ordinary differential equations. Some results in this direction, for local conserved charges, can be found in [55, 56]; two further examples to study would be the higher-order equations related to $SU(n)$ Bethe ansatz systems discussed in [57], and the Schrödinger equations for excited states found in [58].

Acknowledgments

We would like to thank Carl Bender, Clare Dunning, Chris Howls, Frieder Kleefeld, Junji Suzuki, André Voros and Miloslav Znojil for useful conversations and correspondence. RT thanks the EPSRC for an Advanced Fellowship. This work was partly supported by the EC network “EUCLID”, contract number HPRN-CT-2002-00325, and partly by a NATO grant PST.CLG.980424. PED was also supported in part by a JSPS/Royal Society grant and by the Daiwa Foundation, and thanks SPhT Saclay for hospitality while this project was in progress.

References

- [1] C.M. Bender and S. Boettcher, ‘Real Spectra in Non-Hermitian Hamiltonians Having \mathcal{PT} Symmetry’, Phys. Rev. Lett. **80** (1998) 5243–5246 [arXiv:physics/9712001].
- [2] D. Bessis and J. Zinn-Justin, unpublished.
- [3] E. Caliceti, S. Graffi and M. Maioli, ‘Perturbation theory of odd anharmonic oscillators’, Commun. Math. Phys. **75** (1980) 51–66.
- [4] V. Buslaev and V. Grecchi, ‘Equivalence of unstable anharmonic oscillators and double wells’, J. Phys. A **26** (1993) 5541–5549.
- [5] C.M. Bender, S. Boettcher and P.N. Meisinger, ‘ \mathcal{PT} -Symmetric Quantum Mechanics’, J. Math. Phys. **40** (1999) 2201–2229 [arXiv:quant-ph/9809072].
- [6] M. Znojil, ‘ \mathcal{PT} -symmetric harmonic oscillators’, Phys. Lett. A **259** (1999) 220–223 [arXiv:quant-ph/9905020].

- [7] C.M. Bender, S. Boettcher, H.F. Jones and V.M. Savage, ‘Complex Square Well – A New Exactly Solvable Quantum Mechanical Model’, *J. Phys. A* **32** (1999) 6771–6781 [arXiv:quant-ph/9906057].
- [8] P. Dorey and R. Tateo, ‘On the relation between Stokes multipliers and the T-Q systems of conformal field theory’, *Nucl. Phys. B* **563** (1999) 573–602 [Erratum-ibid. B **603** (2001) 581] [arXiv:hep-th/9906219].
- [9] C.M. Bender, M. Berry, P.N. Meisinger, Van M. Savage and M. Simsek, ‘Complex WKB analysis of energy-level degeneracies of non-Hermitian Hamiltonians’, *J. Phys. A* **34** (2001) L31–L36.
- [10] P. Dorey, C. Dunning and R. Tateo, ‘Spectral equivalences, Bethe ansatz equations, and reality properties in \mathcal{PT} -symmetric quantum mechanics’, *J. Phys. A* **34** (2001) 5679–5704 [arXiv:hep-th/0103051].
- [11] P. Dorey, C. Dunning and R. Tateo, ‘Supersymmetry and the spontaneous breakdown of \mathcal{PT} symmetry’, *J. Phys. A* **34** (2001) L391–L400 [arXiv:hep-th/0104119].
- [12] C.W. Bernard and V.M. Savage, ‘Numerical simulations of \mathcal{PT} -symmetric quantum field theories’, *Phys. Rev. D* **64**, 085010 (2001) [arXiv:hep-lat/0106009].
- [13] Z. Yan and C.R. Handy, ‘Extension of a spectral bounding method to the \mathcal{PT} -invariant states of the $-(iX)^N$ non-Hermitian potential’, *J. Phys. A* **34** (2001) 9907–9922.
- [14] K.C. Shin, ‘On the reality of the eigenvalues for a class of \mathcal{PT} -symmetric oscillators’, *Commun. Math. Phys.* **229** (2002) 543–564 [arXiv:math-ph/0201013].
- [15] A. Sinha and R. Roychoudhury, ‘Isospectral partners for a complex \mathcal{PT} -invariant potential’, *Phys. Lett. A* **301** (2002) 163–172.
- [16] A. Mostafazadeh, ‘PseudoHermiticity versus \mathcal{PT} symmetry. The necessary condition for the reality of the spectrum’, *J. Math. Phys.* **43** (2002) 205–214.
- [17] M. Znojil and G. Levai, ‘The interplay of supersymmetry and PT symmetry in quantum mechanics: a case study for the Scarf II potential’, *J. Phys. A* **35** (2002) 8793–8804.
- [18] B. Bagchi and C. Quesne, ‘Non-Hermitian Hamiltonians with real and complex eigenvalues in a Lie-algebraic framework’, *Phys. Lett. A* **300** (2002) 18–26 [arXiv:math-ph/0205002].
- [19] C.M. Bender, D.C. Brody and H.F. Jones, ‘Complex Extension of Quantum Mechanics’, *Phys. Rev. Lett.* **89**, 270401 (2002) [Erratum-ibid. **92**, 119902 (2004)] [arXiv:quant-ph/0208076].
- [20] C.M. Bender, M.V. Berry and A. Mandilara, ‘Generalized \mathcal{PT} symmetry and real spectra’, *J. Phys. A* **35** (2002) L467–L471.
- [21] O. Yesiltas, M. Simsek, R. Sever and C. Tezcan, ‘Exponential Type Complex and non-Hermitian Potentials in \mathcal{PT} -Symmetric Quantum Mechanics’, *Phys. Scripta* **67** (2003) 472 [arXiv:hep-ph/0303014].
- [22] B. Basu-Mallick, T. Bhattacharyya, A. Kundu and B.P. Mandal, ‘Bound and scattering states of extended Calogero model with an additional \mathcal{PT} invariant interaction’, *Czech. J. Phys.* **54** (2004) 5–12 [arXiv:hep-th/0309136].
- [23] F. Kleefeld, ‘Non-Hermitian quantum theory and its holomorphic representation: Introduction and applications’, [arXiv:hep-th/0408097].

- [24] P. Dorey and R. Tateo, ‘Anharmonic oscillators, the thermodynamic Bethe ansatz, and nonlinear integral equations’, *J. Phys. A* **32** (1999) L419–L425 [arXiv:hep-th/9812211].
- [25] V.V. Bazhanov, S.L. Lukyanov and A.B. Zamolodchikov, ‘Spectral determinants for Schroedinger equation and Q-operators of conformal field theory’, *J. Statist. Phys.* **102** (2001) 567–576 [arXiv:hep-th/9812247].
- [26] J. Suzuki, ‘Functional relations in Stokes multipliers – Fun with $x^6 + \alpha x^2$ potential’, *J. Statist. Phys.* **102** (2001) 1029–1047 [arXiv:quant-ph/0003066].
- [27] P. Dorey, C. Dunning and R. Tateo, ‘Ordinary differential equations and integrable models’, *JHEP Proceedings PRHEP-tmr 2000/034, Nonperturbative Quantum Effects 2000*, [arXiv:hep-th/0010148].
- [28] R.J. Baxter, *Exactly solved models in statistical mechanics* (Academic Press 1982).
- [29] V.V. Bazhanov, S.L. Lukyanov and A.B. Zamolodchikov, ‘Integrable Structure of Conformal Field Theory II. Q-operator and DDV equation’, *Commun. Math. Phys.* **190** (1997) 247–278 [arXiv:hep-th/9604044].
- [30] A. Klümper, M.T. Batchelor and P.A. Pearce, ‘Central charges of the 6- and 19-vertex models with twisted boundary conditions’, *J. Phys. A* **24** (1991) 3111–3133.
- [31] C. Destri and H.J. De Vega, ‘Unified approach to thermodynamic Bethe Ansatz and finite size corrections for lattice models and field theories’, *Nucl. Phys. B* **438** (1995) 413–454 [arXiv:hep-th/9407117].
- [32] D. Fioravanti, A. Mariottini, E. Quattrini and F. Ravanini, ‘Excited state Destri-De Vega equation for sine-Gordon and restricted sine-Gordon models’, *Phys. Lett. B* **390** (1997) 243–251 [arXiv:hep-th/9608091].
- [33] V.V. Bazhanov, S.L. Lukyanov and A.B. Zamolodchikov, ‘On nonequilibrium states in QFT model with boundary interaction’, *Nucl. Phys. B* **549** (1999) 529–545 [arXiv:hep-th/9812091].
- [34] C. Destri and H.J. de Vega, ‘Non-linear integral equation and excited-states scaling functions in the sine-Gordon model’, *Nucl. Phys. B* **504** (1997) 621–664 [arXiv:hep-th/9701107].
- [35] P. Dorey and R. Tateo, ‘Excited states by analytic continuation of TBA equations’, *Nucl. Phys. B* **482** (1996) 639–659 [arXiv:hep-th/9607167].
- [36] V.V. Bazhanov, S.L. Lukyanov and A.B. Zamolodchikov, ‘Integrable structure of conformal field theory, quantum KdV theory and thermodynamic Bethe ansatz’, *Commun. Math. Phys.* **177** (1996) 381–398 [arXiv:hep-th/9412229].
- [37] D. Fioravanti and M. Rossi, ‘Exact conserved quantities on the cylinder. I: Conformal case’, *JHEP* **0307** (2003) 031 [arXiv:hep-th/0211094].
- [38] G. Feverati and P. Grinza, ‘Integrals of motion from TBA and lattice-conformal dictionary’, [arXiv:hep-th/0405110].
- [39] V.V. Bazhanov, S.L. Lukyanov and A.B. Zamolodchikov, ‘Quantum field theories in finite volume: Excited state energies’, *Nucl. Phys. B* **489** (1997) 487–531 [arXiv:hep-th/9607099].
- [40] M.V. Berry, ‘Uniform asymptotic smoothing of Stokes’s discontinuities’, *Proc. R. Soc. Lond. A* **422** (1989) 7–21.

- [41] R.M. Corless, G.H. Gonnet, D.E.G. Hare, D.J. Jeffrey and D.E. Knuth, ‘On the Lambert W function’, *Adv. Comp. Math.* **5** (1996) 329–359.
- [42] R.E. Langer, ‘On the connection formulas and the solutions of the wave equations’, *Phys. Rev. D* **51** (1937) 669–676.
- [43] G. Feldman, T. Fulton and A. Devoto, ‘Energy Levels And Level Ordering In The WKB Approximation’, *Nucl. Phys. B* **154** (1979) 441–462.
- [44] M. Seetharaman and S.S. Vasan, ‘Higher-order JWKB approximation for radial problems: III. The r^{2m} oscillator’, *J. Phys. A* **18** (1985) 1041–1045.
- [45] C.M. Bender and S.A. Orszag, *Advanced Mathematical Methods for Scientists and Engineers* (Springer, 1999).
- [46] J.L. Dunham, ‘The Wentzel-Brillouin-Kramers Method of Solving the Wave Equation’, *Phys. Rev.* **41** (1932) 713–720.
- [47] C.M. Bender, K. Olaussen and P.S. Wang, ‘Numerological Analysis Of The WKB Approximation In Large Order’, *Phys. Rev. D* **16** (1977) 1740–1748.
- [48] L.D. Landau and E.M. Lifshitz, *Course of theoretical physics. Vol. 3, Quantum mechanics : non-relativistic theory* (Oxford: Pergamon Press, 1958).
- [49] F. Calogero, *Variable phase approach to potential scattering* (Academic Press, 1967).
- [50] G.E. Andrews, R. Askey and R. Roy, *Special Functions* (Cambridge University Press, 1999).
- [51] M.V. Berry and C.J. Howls, ‘Hyperasymptotics for integrals with saddles’, *Proc. R. Soc. Lond. A* **434** (1991) 657–675.
- [52] W.G.C. Boyd, ‘Error bounds for the method of steepest descents’, *Proc. R. Soc. Lond. A* **440** (1993) 493–518.
- [53] A. Voros, ‘The return of the quartic oscillator. The complex WKB method’, *Ann. Inst. Henri Poincaré*, Vol XXXIX (1983) 211–338.
- [54] M. Robnik and V.G. Romanovski, ‘Some properties of WKB series’, *J. Phys. A* **33** (2000) 5093–5104.
- [55] S.L. Lukyanov, E.S. Vitchev and A.B. Zamolodchikov, ‘Integrable model of boundary interaction: The paperclip’, *Nucl. Phys. B* **683** (2004) 423–454 [arXiv:hep-th/0312168].
- [56] E.S. Vitchev, ‘Families of commuting integrals of motion with certain symmetries’, [arXiv:hep-th/0404195].
- [57] P. Dorey, C. Dunning and R. Tateo, ‘Differential equations for general $SU(n)$ Bethe ansatz systems’, *J. Phys. A* **33** (2000) 8427–8442 [arXiv:hep-th/0008039].
- [58] V.V. Bazhanov, S.L. Lukyanov and A.B. Zamolodchikov, ‘Higher-level eigenvalues of Q-operators and Schroedinger equation’, *Adv. Theor. Math. Phys.* **7** (2004) 711–725 [arXiv:hep-th/0307108].